Section II. LARGE-SCALE DYNAMICS

Chapter 14 Rossby Waves

14.1 *Barotropic waves in a uniform-density fluid.* The oceans and atmosphere are neither static nor do they circulate steadily or simply. When disturbed, their fluid undulates in nearly horizontal currents which can oscillate to and fro, or can snake steadily in standing waves. The patterns of flow and concentrations of energy propagate systematically across vast distances. Waves and 'mean' circulation are intermeshed. The disturbance that creates waves may in fact come from within: internal instability leads to time-dependent currents that may be orderly or chaotic. Or, they may follow an event of external forcing, as when gales blow on the surface of the ocean. Following our discussion of motions with smaller scale, this should really be no surprise. Fluids have many degrees of freedom, and most of them wiggle or undulate. What is more of a surprise is that something like a wave exists which moves the whole body of the fluid, top to bottom, and only incidentally involves its upper surface.

Particularly visible are the large-scale north and south meanders of the atmospheric zonal winds which are related to the 'Rossby' or 'planetary' wave. These waves owe their existence to the rotation and spherical shape of the Earth. Much of the energy in weather patterns and the general circulation involves horizontal scales wider than the depth of the atmosphere: they are subject to the constraints of thin geometry and stable stratification described in Chapter 12 and 13. Viewed from the side, a weather system is 100 to 1000 times thinner (vertically) than its width. This extreme thinness, beyond reminding us of the fragile nature of the atmosphere, causes horizontal winds to be stronger than vertical winds in such weather systems. Stable layering of the air, with its great variations in density reinforces this inequality. Identical remarks apply to the ocean, its layering, thinness and long-wave activity. Small-scale internal gravity waves decorate these layers, yet here we are interested in waves of very large scale, that work on vorticity and rotation-induced stiffness of the fluid. In many ways they are unlike familiar waves on the sea surface, or sound or light.

Rossby waves develop where there are large-scale variations in potential vorticity, all of whose components (relative vorticity, stretching and planetary vorticity) can be active. We have in Chap. 13 introduced the basic equations of balance and prediction for quasi-geostrophic fluids. These rely heavily on ideas of vorticity and potential vorticity. In 'playing' with point vortices in two dimensions and witnessing a mesoscale vortex response to stretching effects in three dimensions, we have set the stage for an entirely new aspect of the Earth environment: the potential vorticity variations at a larger scale, even to the scale of the planet. This is a reflection in dynamics of the geography of the Earth: its nearly spherical shape and its landscape of mountains, continental rises and even more extreme topography of its sea-floor. It seems obvious that the shape of the planet should affect winds and ocean currents: yet the elegant way this shape is encoded in the potential vorticity is a wonderful gift of Nature and mathematics.

Beyond their connection with meandering zonal winds, Rossby waves relate to the oceanic 'Gulf Stream', to climate variability propagating from the tropics during ENSO events, to more broadly to the structure of the meridional overturning circulations of both atmosphere and ocean, and the atmospheres of other planets. Their role in shaping the large-scale circulation will be introduced in Chaps. 16 and 17. They are a kind of 'vorticity wave', which occur in other forms in atmosphere and ocean, for example in small-scale instability of a shear layer, and in the vortex of a hurricane.

Barotropic Rossby waves: the simplest case. The development of potential vorticity (PV) in the previous chapter demonstrated the importance of the vertical vorticity balance, even when it reflects the 'stiffness' of the fluid along lines that are not vertical, but instead lie parallel with the Earth's rotation axis. When the thickness, h, of a layer of fluid is constant, then

$$\zeta + f ,$$

the sum of relative- and planetary vorticity, is the active part of the barotropic PV (known as the absolute vorticity). We begin by considering a single layer of incompressible fluid (virtually like water) of constant depth. This idealization is in fact immensely powerful, providing solutions relevant to the more complex environment of the stratified atmosphere and ocean.

Carl-Gustav Rossby, working at MIT in 1939, introduced the useful approximation for middle latitudes, known as the 'beta-plane'. It approximates the spherical Earth locally by a plane tangent to it, allowing simpler mathematics using Cartesian coordinates to replace the full spherical geometry. Far from the tropics, the Coriolis frequency can be approximated as

$$f = 2\Omega \sin(latitude) \approx f_0 + \beta y$$

where y is the north-south position, measured from some mean latitude y_0. There are errors both in the approximation of f and the neglect of the convergence of the meridians, which must be examined carefully.

Let us now use these ideas to construct a basic Rossby wave for a fluid otherwise at rest. The momentum balance gives us equations in both horizontal directions, x (eastward) and y (northward), for the corresponding velocity components u and v. If we ignore frictional effects and set up a wave with purely north-south motion, u = 0, the momentum equations express an east-west force balance between the pressure gradient and the Coriolis force (the geostrophic balance):

$$-fv = -\frac{1}{\rho} p_x$$

and a north-south force balance between acceleration per unit mass, and pressure gradient:

$$v_t = -\frac{1}{\rho} p_y$$

Eliminating the pressure, p, between these two equations gives a wave equation for v:

$$v_{xt} + \beta v = 0 \qquad (14.1)$$

where β = df/dy, approximated as a constant in the equation. Assuming a wave of the form $v = A\cos(kx - \omega t)$ we substitute in the wave equation to find

$$\sigma = -\beta / k$$

This key relation between the *wavenumber* k (which is 2π divided by the wavelength) and the frequency σ tells us that longer waves have higher frequency and that this frequency scales as σ/f ~ L/a, the ratio of the length scale of the wave (k^{-1}) to the Earth's radius a. The propagation speed, c, (the phase speed) is westward relative to the fluid, with magnitude β/k^2. In more familiar wave systems, for example *non-dispersive* sound waves, light waves or waves on a vibrating string, the frequency varies directly with wavenumber and the propagation speed c is a constant. As we encountered with surface gravity waves and internal waves, dispersive waves turn a localized disturbance into long trains of sine-waves with gradually varying wavelength (as from a pebble thrown into a pond). By contrast, non-dispersive waves like sound and radio waves preserve the properties of isolated pulses, making possible communication to a great distance.

If we add a uniform, eastward flow, U, the advective acceleration changes Eqn (14.1) to

$$v_t + Uv_x = -\frac{1}{\rho} p_y ,$$

and the dispersion relation becomes

$$\sigma = Uk - \beta / k \qquad (14.2)$$

as one might have guessed, the frequency is Doppler-shifted by the mean current. The east-west phase speed is

$$c \equiv \sigma / k = U - \beta / k^2 . \qquad (14.3)$$

With $\beta = 0$ a wave is 'frozen' in the fluid (it does not propagate relative to the fluid), and then c = U as we expect. The special case c = 0 is particularly important in the atmosphere, where much of the forcing of the atmosphere is fixed in time or slowly varying. Eqn. (14.3) is Rossby's 'trough formula' describing the propagation speed of idealized long, north-south meanders of the westerly winds. This simple equation, and the more complete theories that preceded it, by Hough, Goldsbrough and particularly Haurwitz, gave meteorologists a new way to think about developing weather. The meandering of jet streams, which are narrow, intense and baroclinic, is not well described by the theory at this stage, but Eqn. (14.3) with c = 0 is still a key limiting case of the more complex problem of stationary waves in the atmospheric circulation and the zonal circulation of the atmosphere and of the great Antarctic Circumpolar Current in the Southern Ocean.

Rossby waves involve fields of pressure and velocity in which the Coriolis force, directly and indirectly (through pressure) produces a restoring force for fluid that moves north or south. Being nearly in geostrophic balance, the pressure is nearly constant along streamlines, yet it is in subtle departures from this balance that pressure can accelerate the flow.

The principle of conservation of PV gives a clearer description of the restoring effect at work in Rossby waves. With a mean westerly wind, air that moves northward in a standing wave pattern, conserving the sum $\zeta + f$ will have to develop negative spin or vorticity, ζ, as it encounters smaller values of f found at high latitude. This anticyclonic spin matches with the northward velocity, west of the parcel, and the southward velocity to its east (Figure 14.1), enforcing the basic wave pattern. In downwind regions where the wave has not yet penetrated, this spin will extend the pattern eastward at twice the speed of the mean westerly wind speed. For fluid initially at rest, with no mean zonal flow, the same dynamics apply, and the graphical argument shows that the north-south velocity induced by the pattern of vorticity in Fig. 14.1 will cause the sinusoidal wave to propagate westward.

Figure 14.1 Showing how a parcel of fluid moved northward in a standing wave, conserving its potential vorticity, $\zeta + f$, develops negative (anticyclonic) spin, ζ, which affects fluid to the east and west, reinforcing the north-south motion of the

wave itself. For the case of a fluid without a mean zonal current, the same argument shows that the pattern propagates westward relative to the fluid.

14.2 *Topographic Rossby waves.* It is essential at this point to give the waves the full freedom of 2- (and later, 3-) dimensions. We begin with the simplest case of a fluid with a bottom slope, on an f-plane (without the spherical β-effect). Vorticity principles formed the derivation of the vertical vorticity equation, written for quasi-geostrophic flows in terms of the free-surface height, η, in Chap. 13 above. Another connection can be made with the familiar long-gravity-wave equations, and the procedure also provides a relatively quick derivation of the final equations of section 13.2. We assume that nonlinear terms can be neglected in both momentum and mass-conservation equations. Making the hydrostatic-pressure approximation, (with or without the small Rossby-number assumption used earlier), the horizontal velocity is independent of z, and the momentum equations become

$$\begin{aligned} u_t - fv &= -g\eta_x \\ v_t + fu &= -g\eta_y \end{aligned} \qquad (14.4)$$

while mass-conservation becomes

$$\eta_t = -((hu)_x + (hv)_y). \qquad (14.5)$$

where h = H + h'(x,y) + η(x,y,t). This is derived by noting that (hu, hv) is the lateral volume transport across a vertical section of the fluid, and flow divergence must be balanced by vertical motion at the free surface (Fig. 14.2).

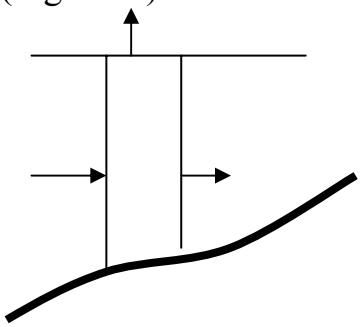

Fig. 14.2 Mass conservation relates horizontal variations of hu to vertical movement of the free surface.

Alternatively, with u and v independent of z,

$$u_x + v_y + w_z = 0$$

we multiply by h, and use the boundary conditions $w=\eta_t$ at z=0 and $w=-uh_x-vh_y$ at z=-h to find the same result. Form $(h(\ (14.4)a))_x+(h((14.4)b))_y$ which is known as a 'divergence' equation, describing the rate of change of the horizontal divergence of volume flux, $\nabla\bullet(h\vec{u})$. Then form $(h(\ (14.4))_y + (h((14.4)b))_x$ which is a vorticity equation. These combine with $+(1/g)(h(\ (14.5))_x)_x + (h(\ (14.5))_y)_y)$ to give

$$[\eta_{tt} + f^2\eta - \nabla\bullet gh\nabla\eta]_t + gfJ(\eta,h) = 0 \qquad (14.6)$$

(see also, e.g. *Pedlosky, Geophysical Fluid Dynamics*, 3.7). Here, as described earlier, J is the Jacobian operator, written in various ways as

$$J(a,b) = a_x b_y - a_y b_x = \nabla a \times \nabla b \bullet \hat{z} = \frac{\partial(a,b)}{\partial(x,y)}$$

Scale analysis of the wave equation. Eqn. (14.6) describes a wealth of waves, with both high-frequency and low-frequency. If the wave frequency is much greater than f, the terms in the first set of brackets, with f =0, give long, hydrostatic, non-dispersive gravity waves. With h=constant, f≠0, Coriolis effects make these waves dispersive and provide a low-frequency cut-off at f. More generally, if T is the time-scale of the waves (T= 1/frequency), and L is their horizontal length scale (L=wavelength/2π), and H the mean depth, then scale analysis of the four terms in the equation gives, respectively:

$$\frac{\eta}{T^3}, \quad \frac{f^2\eta}{T}, \quad \frac{gH\eta}{L^2T}, \quad \frac{H\delta gf\eta}{L^2}$$

where Hδ is the typical size of topographic heights at the scale L. Motions at high frequency (small T) include long gravity waves, with Coriolis effects, and Kelvin waves: in this case the final term in Eqn. (14.6) can be neglected. Yet one can see that a new set of motions with low frequency may be possible by balancing the final term with the 2d or 3d term. In this case, the frequency will be

$$T^{-1} \sim f\delta.$$

For this choice of frequency range, the first term divided by the second term is just $O(\delta^2)$. Evidentally, if the height of the topography (measured over the horizontal wave-scale L). is much smaller than the mean depth, then the first term is negligibly small, leaving the equation

$$[f^2\eta - \nabla \bullet gh\nabla\eta]_t + gfJ(\eta,h) = 0 \qquad (14.7)$$

Let us choose a particular bottom topography, a simple up-slope to the north. Let

$$h = H + h'(x,y) + \eta(x,y,t)$$

with $h' = -\alpha y$. For small amplitude waves, η may be neglected in the expression for h. Then Eqn. (14.7) becomes

$$-(f^2/g)\eta_\tau + h(\eta_{xx} + \eta_{yy} + (h_y/h)\eta_y)_t - fh_y\eta_x = 0$$

$$-(f^2/g)\eta_\tau + (H - \alpha y)(\eta_{xx} + \eta_{yy} - (\alpha/(H-\alpha y))\eta_y)_t + f\alpha\eta_x = 0$$

Scale analysis of this equation gives the following terms:

$$\frac{f^2\eta}{gT} \quad \frac{(H+\alpha L)\eta}{L^2T} \quad \frac{(H+\alpha L)\eta}{L^2T} \quad \frac{\alpha\eta}{LT} \quad \frac{\eta}{L^2T} \quad \frac{f\alpha\eta}{L}$$

Earlier we saw that the topographic height divided by mean depth, δ (= αL/H) had to be small to achieve a balance involving the new topographic term. So here we neglect the small O(αL/H) parts of terms 2 and 3, and similarly neglect term 4 relative to terms 2 and 3, giving

$$(\eta_{xx} + \eta_{yy})_t - (f^2/gH)\eta_\tau + (f\alpha/H)\eta_x = 0 \qquad (14.8)$$

which is the equation for topographic Rossby waves. Its most important property is that it is linear: two solutions added together give a third solution, and initial conditions with a complicated shape in x and y can be expressed as a sum of many Fourier components. Eqn. (14.8) has constant coefficients and thus will yield simple solutions for propagating plane waves.

Some Mathematical Background. How does this equation compare with those of classical physics? Linear second-order pde's (partial differential equations) fall into three groups, *hyperbolic (e.g., the classic wave equation), elliptic (e.g., Laplace's equation)* and *parabolic (e.g. the heat-diffusion equation).* The classic wave equation for vibrating strings and membranes, long gravity waves on water and sound waves is hyperbolic with respect to space and time,

$$\eta_{xx} + \eta_{yy} - c_0^{-2}\eta_{tt} = 0 .$$

Wave-like solutions η = Real(Aexp(ikx + ily - iσt), after substitution in the equation, yield the *dispersion relation*

$$\sigma^2 = c_0^2(k^2 + l^2)$$

for which the phase speed, $\sigma/(k^2 + l^2)^{1/2}$ is independent of both *wavelength* and *direction* of propagation. That is, the waves are both *non-dispersive* and *isotropic.* The equation has characteristic curves, along which solutions propagate. Isolated, pulse-like initial conditions (a stone thrown in a pond) are prevented from dispersing into sinusoidal waves…Fourier components. A top-hat like wave can propagate without change of shape along a vibrating string; in two-dimensions it will decay in amplitude as it spreads out in a ring (leaving a narrow wake). The stone thrown in a pond of course excites short gravity waves and even shorter surface-tension waves (ripples), which disperse into sine-wave trains. Text-books on waves are usually divided neatly into two sections: dispersive and non-dispersive waves, because the solutions and techniques for solving them differ so greatly (e.g., Lighthill's text, *Waves in Fluids,* 1978, Whitham, *Linear and Nonlinear Waves,* Addison-Wesley 1974).

Eqn. (14.8) does not fall neatly into one of these three categories, because it is formally a third-order pde. However here (and with the classical wave equation), the time-variable is separable. Assuming sinusoidal time-dependence the remaining equation is of 2d order and elliptic in space variables x and y. This too occurs when an exp(-iσt) factor is separated from the classic wave equation, leaving the *Helmholtz equation,*

$$\nabla^2\eta + (c_0^2/\sigma^2)\eta = 0 .$$

Elliptic pde'sk typically require boundary conditions 'all-around', for example on a boundary surrounding the fluid, for the solutions to be well-determined. Solutions however are readily found, both plane waves and for waves generated at a single point in space. These latter are 'Green's functions', a sort of 'impulse response' for the wave equation, and are useful in building intuition for cause and effect in fluids.

Topographic Rossby wave solutions. Consider solutions in the form of a plane wave,

$$\begin{aligned}\eta &= \mathrm{Re}(A\exp(ikx + ily - i\sigma t)\\ &= \mathrm{Re}(A\exp(i\vec{k}\bullet\vec{x} - i\sigma t))\\ &= \mathrm{Re}(A\exp(i\theta(x,y,t))\end{aligned}$$

'Re(_)' denotes the real part. The *wavevector* $\vec{k} = (k,l)$ with its scalar *wavenumber* components k and l, is perpendicular to the wave crests, which are lines of constant *phase, θ(x,y,t).* Substituting in the wave equation, the physics of the problem boils down to the *dispersion relation*, connecting the wavenumbers and frequency.

$$\sigma = -(f\alpha / H)\frac{k}{k^2 + l^2 + 1/\lambda_{BT}^2} \qquad (14.9)$$

where $\lambda_{BT} = (gH)^{1/2}/f$ is the Rossby deformation radius. Note that

$$\lambda_{BT} = c_0/f$$

where c_0 is the propagation speed of long gravity waves (with f=0); this definition of the 'Rossby radius' turns out to be valid under much more general circumstances. Because η does not vary along the wave-crests, along which the phase θ is constant, the horizontal velocity of the fluid lies nearly along the crests. This is suggested by geostrophic balance (because the pressure gradient is nearly parallel with $\vec{k}$. Or, the mass-conservation equation , $u_x + v_y = 0 + O(\delta)$, also suggests the same thing, because when u and v are expressed in terms of the wave-like η, we have $i\vec{k} \bullet \vec{u} = 0 + O(\delta)$, again saying that the velocity lies nearly along the wave-crests.

The dispersion relation, σ as a function of k and l (Fig. 14.3) is shaped like a 'witch's hat', peaking near the origin. Height contours of σ(k,l), show possible wave-vectors for a constant σ. These are circles tangent to the l-axis (see also Fig. 14.10).

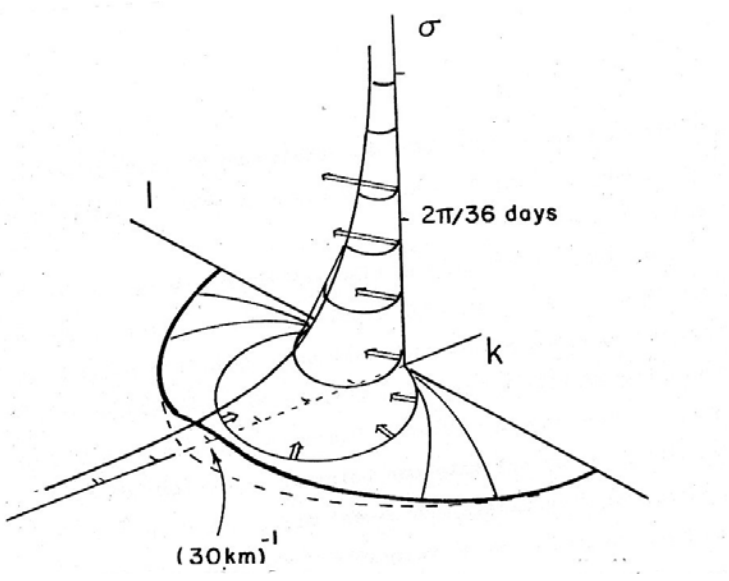

Fig. 14.3 Frequency σ as a function of wavenumbers (k,l) for topographic Rossby waves. The highest frequencies arise for the longest waves, near the origin. σ is constant along the solid circular curves. The group velocity (double arrows) points inward toward the centers of these circles.

Waves in a channel. A complete mathematical problem consists of both equation and boundary conditions. Here we add vertical walls to the topographic wave problem, at which the normal fluid velocity must vanish. Thus suppose

$$v = 0 \text{ at } y = 0, L .$$

The momentum equations show that $v = (g/f)\eta_x + O(1/fT)$, so we will simply require that η_x vanishes at the two east-west running boundaries of the channel. This will be achieved by the separable solution

$$\eta = A \sin ly \exp(ikx - i\sigma t)$$

if we choose y-wavenumbers, $l = n\pi/L$, for n = 1, 2,…. . The dispersion relation becomes

$$\sigma = -(f\alpha / H)\frac{k}{k^2 + n^2\pi^2 / L^2 + 1/\lambda_{BT}^2}$$

The frequency rises to a maximum at $k^2 = n^2\pi^2 / L^2 + 1/\lambda_{BT}^2$, falling toward zero for both longer and shorter waves. The curve is a cut through the two-dimensional Fig. 14.3, at fixed north-south wavenumber, l. Notice that the wave pattern always moves toward negative x (westward in this case), for $\sigma/k < 0$. However the group velocity along the channel, $\partial\sigma/\partial k$, can take either sign; it is the *slope* of the $\sigma(k)$ curve for a fixed value of n. Energy propagates westward in the longer waves and eastward in the shorter waves.

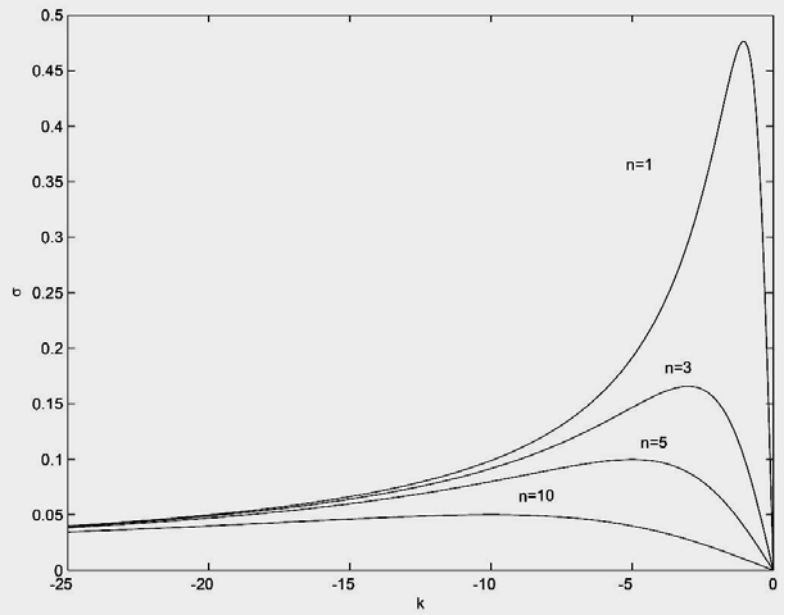

Fig. 14.4 Topographic Rossby wave dispersion relation $\sigma(k)$ for various north-south modes, n. All waves have $k<0$, and the longer waves to the right of the frequency maximum become non-dispersive in the x-direction as their wavelength increases.

There are several interesting limiting cases. For the shorter waves (that is, with large wavenumber)

$$\sigma = -f\alpha H / k;$$

the frequency varies inversely with k. For the longest waves, as k =>0,

$$\sigma = \frac{-f\alpha / H}{n^2 / L^2 + \lambda_{BT}^{-2}} k$$

the waves are non-dispersive; all waves in a single mode, n, and in this long-wave limit, propagate at the same speed, westward along the channel. These waves have k << l, so that the gradient of the free-surface height, $\nabla\eta$, points nearly across the channel (north/south), and the oscillating velocity field is directed nearly along the channel, u >> v. For this example we have kept the Rossby Radius, λ_{BT}, large compared with the channel width, L. If this were not so we would have a larger regime of non-dispersive waves moving west along the channel, in fact all wavenumbers obeying $(k^2 + l^2)^{1/2} \lambda << 1$ are non-dispersive. Eqn. (14.8), for this case, L >> λ_R, simplifies to a remarkably simple 1st order pde:

$$\eta_\tau - (g\alpha / f)\eta_x = 0 \qquad (14.10)$$

The general solution of this wave equation is westward propagation without change of shape: $\eta = m(x + (g\alpha/f)t)$, for an arbitrary function m(•).

14.3 *'True' Rossby waves on a spherical Earth.* The discussion of potential vorticity dynamics in the previous chapter showed the importance of the vertical component of the planetary vorticity, $2\Omega \sin\varphi \equiv f$, and its variation with latitude, which produces effects analogous to the topographic restoring effect and waves described above. We now return to the more general case of a spherical Earth (of course the Earth has an equatorial bulge, and hence more closely approximates an ellipsoid with complex topography superimposed on it. Given that the smoothed geoid deviates from a sphere, the radius in the Equatorial plane being about about 21 km greater than the radius to either pole; the mean radius, a, is about 6380 km. We shall neglect the difference). The momentum equations in spherical coordinates (λ,φ,r) are similar to their Cartesian (x,y,z) counterparts. Notation varies among different texts but here we let λ be longitude (positive eastward), φ be latitude (positive northward) and r radius (equivalent to a + z). Corresponding velocity components are (u,v,w). They are derived in ¤Gill, secs. 4.12, 11.2. Ignoring nonlinear terms, and setting the vertical velocity, w, to zero for this homogeneous fluid we have

$$\begin{aligned}
&\frac{\partial u}{\partial t} - 2\Omega \sin\varphi\, v = -\frac{g}{a\cos\varphi}\frac{\partial \eta}{\partial \lambda} \\
&\frac{\partial v}{\partial t} + 2\Omega \sin\varphi\, u = -\frac{g}{a}\frac{\partial \eta}{\partial \varphi} \qquad (14.11) \\
&\frac{\partial \eta}{\partial t} + \frac{1}{a\cos\varphi}\left\{\frac{\partial}{\partial \lambda}(hu) + \frac{\partial}{\partial \varphi}(hv\cos\varphi)\right\} = 0
\end{aligned}$$

Here $\frac{1}{a\cos\varphi}\frac{\partial(\bullet)}{\partial\lambda}$ plays the role of $\frac{\partial}{\partial x}$ because as the constant longitude meridians converge towards the pole, the scale factor (r cos φ) relates longitude to east-west distance. Similarly the (r φ) = y, the north-south distance. We have made the 'thin-shell' approximation, replacing r by

its average value a. In two places we have neglected the horizontal component of $\vec{\Omega}$, which is known as the 'traditional approximation': the x-momentum balance and the vertical momentum balance, which is assumed hydrostatic as usual; scale analysis shows that the approximation involves errors of order $\varepsilon\left(\frac{H}{L}\right)^2 \cot\varphi$ and hence is adequate for the unless one is close to the Equator; it relates to whether the fluid moves in columns that remain parallel to $\vec{\Omega}$ or parallel to the local vertical direction. As one sees in laboratory experiments, shear layers can form in this fluid along cylinders that touch the inner sphere at the Equator. In Batchelor's *Introduction to Fluid Dynamics (1967),* Appendix 2¤ gives a useful discussion of coordinate systems and corresponding vorticity and divergence expressions. The easiest way to derive these expressions is to draw a small area element bounded by constant circles of latitude and longitude, and work out the volume inflow through the faces of this area (for divergence) and (for vorticity) the circulation $\vec{u} \bullet d\vec{l}$ integrated around its edges (where $d\vec{l}$ is a vector line segment marking the boundary of this elemental area). This integral is equal to the product of area of the element and vertical vorticity, by Stokes' theorem.

For simplicity consider the time-mean depth h to be constant. The curl of the momentum equations gives

$$\begin{aligned}
&\zeta_t + (f/a\cos\varphi)(u_\lambda + (v\cos\varphi)_\varphi) + \beta v = 0 \\
&\zeta = (1/a\cos\varphi)(v_\lambda - (u\cos\varphi)_\varphi) \\
&\quad = (g/2\Omega\sin\varphi)\Delta\eta \quad \textit{where} \\
&\Delta\eta \equiv \{\frac{1}{a^2\cos^2\varphi}\frac{\partial^2}{\partial\lambda^2} + \frac{1}{a^2\cos\varphi}\frac{\partial}{\partial\varphi}(\cos\varphi\frac{\partial}{\partial\varphi})\}\eta
\end{aligned} \qquad (14.12)$$

Recognize that the second term in eqn. (14.12)a contains the horizontal divergence ($u_x + v_y$ in Cartesian coordinates). Using the mass conservation equation (14.11)c, the vorticity equation becomes

$$\frac{\partial}{\partial t}\Delta\eta - ((2\Omega\sin\varphi)^2/gH)\frac{\partial\eta}{\partial t} + \frac{2\Omega}{a^2}\frac{\partial\eta}{\partial\lambda} = 0, \qquad (14.13)$$

which may also be written

$$\frac{\partial}{\partial t}\Delta\eta - (f^2/gH)\frac{\partial\eta}{\partial t} + \frac{\beta}{a\cos\varphi}\frac{\partial\eta}{\partial\lambda} = 0$$

where $f = 2\Omega \sin\varphi$, and $\beta = (2\Omega/a)\cos\varphi$ is the northward derivative of Coriolis frequency, f. Here the horizontal Laplacian in spherical coordinates is written $\Delta\eta$. This is the close analogue of Eqn. (14.8), for topographic Rossby waves over a plane bottom slope, as the second version of the equation shows plainly. The full spherical problem, though complicated by the geometry, has a simple physical essence. Eqn. (14.13) has elegant solutions on the sphere, described by Longuet-Higgins (1964). One feature to note is that by looking for solutions that propagate westward without change of form, or equivalently going to a reference frame that rotates more

slowly than the Earth, the wave equation in the non-divergent limit, $L/\lambda_R << 1$, becomes simplified. Try a solution of the form $\eta(\lambda,\varphi,t) = \tilde{\eta}(\lambda + c_1 t, \varphi)$, and (14.13) becomes,

$$\Delta\tilde{\eta} + \frac{2\Omega}{c_1 a^2}\tilde{\eta} = 0$$

which is Helmholtz's equation with a constant coefficient, giving the spatial form of sinusoidal (in time) oscillations of a spherical membrane. The value of such statements is that we can imagine elastic waves and this provides some confidence in the existence of Rossby waves! The β-plane version of this statement is simply that all Rossby waves of the same wavelength (yet propagating in many different directions), have the same westward phase speed, and hence appear stationary to an observer moving westward at that speed.

Both topographic Rossby waves and 'true' Rossby waves originate in the conservation of potential vorticity for a homogeneous fluid, as we describe in the next section.

Potential vorticity (PV) description of Rossby waves.. The Rossby wave equation is an expression of the conservation of PV for small-amplitude, low-frequency motions. The PV expression for uniform mean depth, linear Rossby waves, is

$$\frac{D(\zeta + f - f\eta/H)}{Dt} = 0 \qquad (14.14)$$

which is found by substituting for $\partial\eta/\partial t$ in eqn. (14.13), using mass conservation, eqn (14.11)c. In spherical coordinates the time-rate of change following the fluid is written ¤

$$\frac{D}{Dt} = \frac{\partial}{\partial t} + \frac{u}{a\cos\varphi}\frac{\partial}{\partial\lambda} + \frac{v}{a}\frac{\partial}{\partial\varphi}$$

It is straight-forward to derive the most exact and general form of potential vorticity conservation. Kelvin's circulation theorem, or equivalently the radial ('vertical') vorticity equation, shows that, following inviscid motion of a constant-density fluid,

$$\frac{Dq}{Dt} = 0; \qquad q = \frac{f+\zeta}{h} = \frac{absolute\ vorticity}{h} \qquad (14.15)$$

This was discussed at the end of Chapter 13. It is equivalent to conservation of the absolute angular momentum of a small disk of fluid lying horizontal (parallel with the surface of the sphere) provided that the disk has circular cross-section. As the thickness h of the disk increases, its horizontal area decreases in proportion, and with a decreased moment of inertia, it spins faster (as seen by a non-rotating observer 'off' the planet). Fluids deform, however, so that for fluids, potential vorticity conservation is a more general and far-reaching principle, than

angular momentum conservation. Eqn. (14.14) is a small-amplitude approximation to (14.15), with $h = H+\eta$.

There are some subtleties. As the fluid moves on the sphere, this formulation assumes that a small horizontal disk of fluid will remain nearly horizontal. By making its width L much greater than the depth, h, this is a good approximation for a 'thin' ocean on a sphere. However, we earlier gave an argument for steady circulations that invoked the 'stiffness' of the rotating fluid along lines parallel with the rotation axis. This gave the correct results for slow circulations, as governed by the 'Sverdrup relation' yet would give the wrong answer for Rossby waves. The thin spherical shell 'wins' over the 'stiff column' constraint, provided that the motions indeed are much broader than the depth of the fluid. If we derive the Rossby wave dispersion relation assuming columns parallel to $\vec{\Omega}$ remain parallel as they move north or south, it is grossly in error, as a disk of fluid initially horizontal would not under this assumption remain horizontal enough as it moves. In a confusing situation like this one can look to laboratory experiments for help. In a rotating experiment with homogeneous-density fluid in a spherical shell, the 'stiff columns' which form parallel with the axis of rotation cause peculiar dynamical effects near the Equator, particularly with a cylindrical shear layer oriented parallel to $\vec{\Omega}$, hence nearly horizontal for observers near the Equator. These effects come from Coriolis terms neglected in eqn. (5.6) where it was assumed that w=0. Neglect of the horizontal component of $\vec{\Omega}$ is known as the 'traditional approximation', and it relies on the thinness of the spherical shell, which singles out the vertical component of the Earth's rotation vector.

14.4 *The β-plane.* For Rossby waves with length scale $(k^2 + l^2)^{-1/2}$ smaller than the Earth's radius, we can approximate the spherical coordinates by Cartesian coordinates in a plane tangent to the sphere as suggested in Sec. 14.1. This was Rossby's (1939) brilliant insight, which gave meteorology a strong and useful theory of the waves in the westerly winds. Thus writing $dy = a\, d\varphi$ and $dx = a \cos\varphi\, d\lambda$, we return exactly to Eqn. (14.8),

$$(\eta_{xx} + \eta_{yy})_t - (f^2/gH)\eta_\tau + \beta\eta_x = 0 \qquad (14.16)$$

where β takes over the role of the bottom slope, $f\alpha/H$. This is the β-plane equation for Rossby waves. It has three forms: for the *mid-latitude β-plane*, f is taken to be constant (except where differentiated), equal to $2\Omega \sin\varphi_0$, where φ_0 is the central latitude of the region of interest. β is likewise taken to be constant, $2\Omega \cos\varphi_0/a$. Errors in making this approximation are typically of order L/a. For the *polar β-plane* one adopts a cylindrical geometry centered on the North or South Pole, and f is expanded in a Taylor series, as $f = f_0 - \frac{1}{2}(\frac{r}{a})^2$ where r is distance from the pole. For the *equatorial β-plane*, our origin for y is the Equator itself, and we take

$$f \cong \beta y = 2\Omega y/a$$

so that $\beta = 2\Omega/a$, again a constant. Notice that now the vorticity equation (14.16) has a non-constant coefficient, proportional to y^2. This makes it the Schrödinger equation of quantum mechanics, and suggests the 'potential well' solution known as the parabolic oscillator. Indeed, the Equator is a wave-guide not unlike the channel model derived for Eqn. (14.8). Waves propagate along the Equator while being trapped north-south by the increase of the Coriolis frequency, with latitude. Because the convergence of the meridians of longitude is slightest at

the Equator, the equatorial β-plane is a more accurate approximation ($O(L/a)^2$) than the mid-latitude β-plane (O(L/a)), which is a reason for being familiar with the full spherical form of the equation. We should note that the equatorial region has a crucially important Kelvin-wave mode which is missed by this low-frequency analysis, yet can be recovered by going back to the equatorial version of equation (14.6). Equatorial waves are discussed further at the end of this chapter.

The non-divergent approximation and introduction of the stream-function. For waves with length scale much smaller than the (external) Rossby deformation radius, $L << \lambda$, the 'free-surface' term in the wave equation (14.16) can be neglected. At the same time, the pressure and free-surface elevation are nearly proportional, and both act as a stream function for the horizontal velocity, with accuracy of order Rossby number, ε (see Chap. 12),

$$\vec{u} \equiv \vec{z} \times \nabla \psi$$

In this limit the Rossby wave equation is

$$(\psi_{xx} + \psi_{yy})_t + \beta \psi_x = 0 \qquad (14.17)$$

14.5 *Energy propagation and wave-packets: review of group velocity.* A property of dispersive waves is that their energy does not generally move with the individual wave-crests. Surface gravity waves are a familiar example, discussed in Sec. I of this text, in which the wave groups or wave 'packets' move with ½ the speed of wave-crests. This means, for example that you can surf on the wake of a ferry-boat, because the narrow 'vee-shaped' wake is comprised of individual wave-crests that move forward through the wave-packet, increasing in size and then disappearing at its leading edge. There is a continual supply of new waves to lengthen your ride. The basic phenomenon is evident in just two sinusoidal wave components of the form $\eta = \sin(kx - \sigma t)$, with slightly different wavelengths, which together produce an interference pattern, wave-packets well-separated by nearly still water,

$$\eta = \sin(k_1 - \delta k)x + \sin(k_1 + \delta k)x = 2\sin(k_1 x)\cos(\delta k\ x)$$

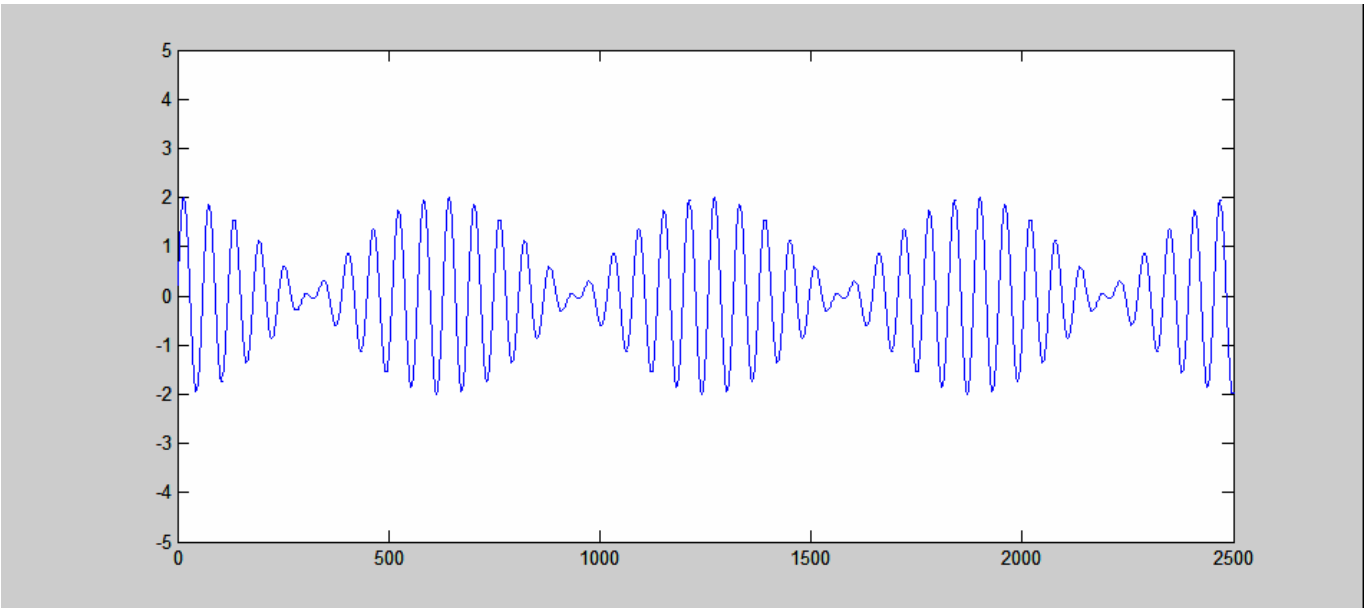

Fig. 14.5 Wave packets formed by adding just two sinusoidal Fourier components. Individual waves move with the phase speed, while the groups move with the group velocity.

The number of waves in each packet is approximately 10 in this example, and this is just equal to $\frac{1}{2}k_1/\delta k$. Now consider the propagation of the pattern with time. With

$$\sigma(k_1+\delta k)=\sigma(k_1)+\delta k\frac{\partial\sigma}{\partial k}+O((\delta k)^2) \text{ we have}$$

$$\eta(x,\tau)=\sin((k_1-\delta k)x-(\sigma-\sigma_k\delta k)t)+\sin(k_1+\delta k)x-(\sigma+\sigma_k\delta k)t)=2\sin(k_1x)\cos(\delta k\,(x-\sigma_k t))$$

which is shown in a contour plot in Fig. 14.6.

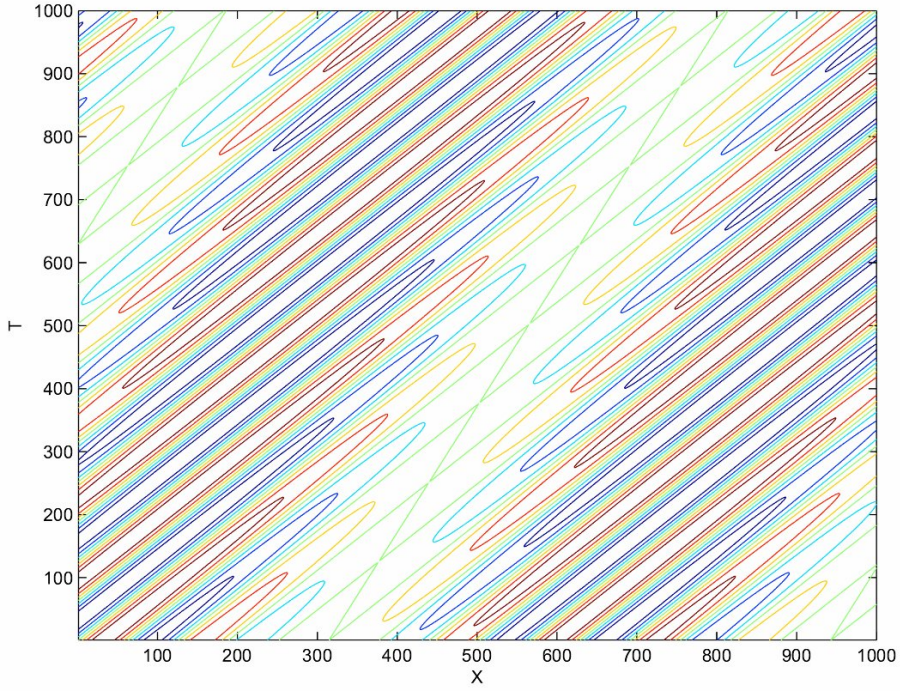

Fig. 14.6 *x-t* (Hoevmueller-) diagram showing wave-packets propagating to the right (time increases upward). Here we chose the group velocity to be ½ the phase velocity, as with short surface gravity waves; dX/dt is inverse to the slopes seen, so that the wave-crests move twice as rapidly as the wave-packets. Each moving group could be the wake behind a moving boat.

This pattern can be animated 'by hand', after copying Fig. 14.7 once on a transparency and once on white paper. Line up the two figures with the black bars ('wave-crests') parallel, and slide them apart, keeping the bars parallel. The interference pattern moves at a speed different than the speed of the individual wave-crests. Notice that the figure has a slowly varying wavelength from top to bottom. The group velocity, c_g, of the wave-packets, relative to phase speed, c, depends on whether the longer wave has faster or slower c; this will change as the patterns are moved apart. The relevant formula is, for propagation in one dimension, $\sigma=ck$,

$$c_g = \frac{\partial \sigma}{\partial k} \equiv c + k\frac{\partial c}{\partial k} \tag{14.18}$$

As the sheets are displaced relative to one another, the movement of the interference pattern depends on whether the longer wave has faster or slower speed, c, than the shorter wave. Notice that as you hold the transparent sheets you are 'moving with the average speed of the wave-crests' so that it is the final term $k\partial c/\partial k$ that is at work in moving the interference pattern.

Rossby-wave group velocity. In two or three dimensions, energy propagates with the vector group velocity, $\vec{c}_g = (\frac{\partial \sigma}{\partial k}, \frac{\partial \sigma}{\partial l})$. This is the gradient of the function $\sigma(k,l)$ which is drawn with arrows on Fig. 5.2, perpendicular to the curves of constant frequency, pointing inward toward high frequency. Differentiating the dispersion relation we find

$$\begin{aligned} \vec{c}_g &= \beta \frac{(k^2 - l^2 - \lambda^{-2}, 2kl)}{(k^2 + l^2 + \lambda^{-2})^2} \\ &= \beta K^2 \frac{(\cos 2\mu - \lambda^{-2}, \sin 2\mu)}{(K^2 + \lambda^{-2})^2} \end{aligned} \tag{14.19}$$

where polar coordinates have been introduced, $(k,l) = K(\cos \mu, \sin \mu)$. For waves much shorter than the Rossby radius, $1/\lambda^2$ can be neglected and the group velocity has a magnitude β/K^2 $(=\sigma/k)$ and direction 2μ.

The fact that the group velocity for anisotropic waves is not directed parallel with $\vec{k}$ can be seen using the Moiré pattern transparency. Hold the two sheets so that the bars are no longer parallel, and the interference bands (the energy) will move at a steep angle to the wave crests. Again remember that as you hold the figure you are 'moving with the phase velocity c'. The movement of the interference bands tells us one component of the group velocity; to see both components one can take three such sheets (at least two being transparent) and form 2-dimensional wave-packets. Moving them according to the 'rules' of the dispersion relation demonstrates the full vector group velocity (though it requires some dexterity!).

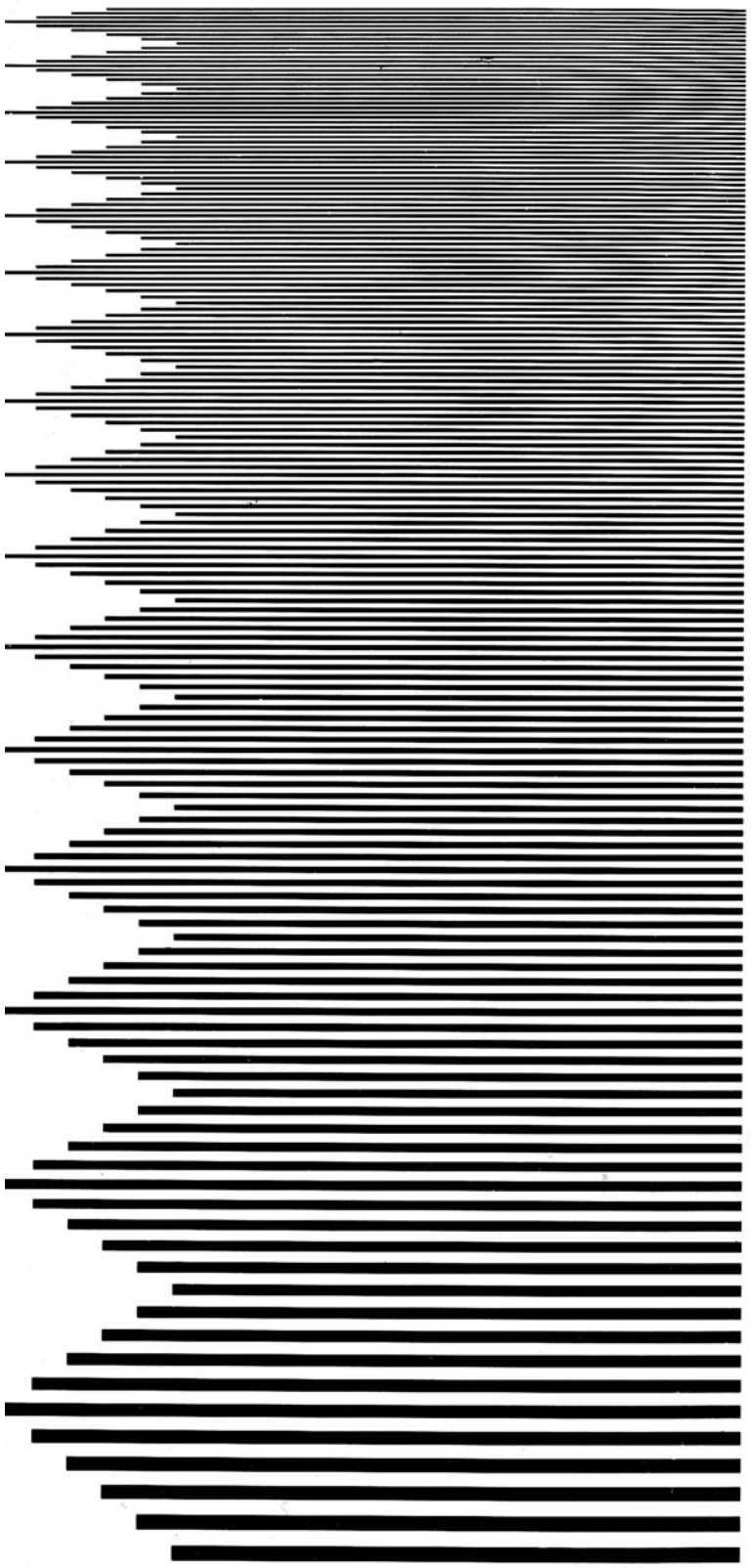

Fig 14.7 When this figure is copied onto a transparency, and a second copy on white paper, superposing the two will generate moving wave-packets as Moiré patterns.

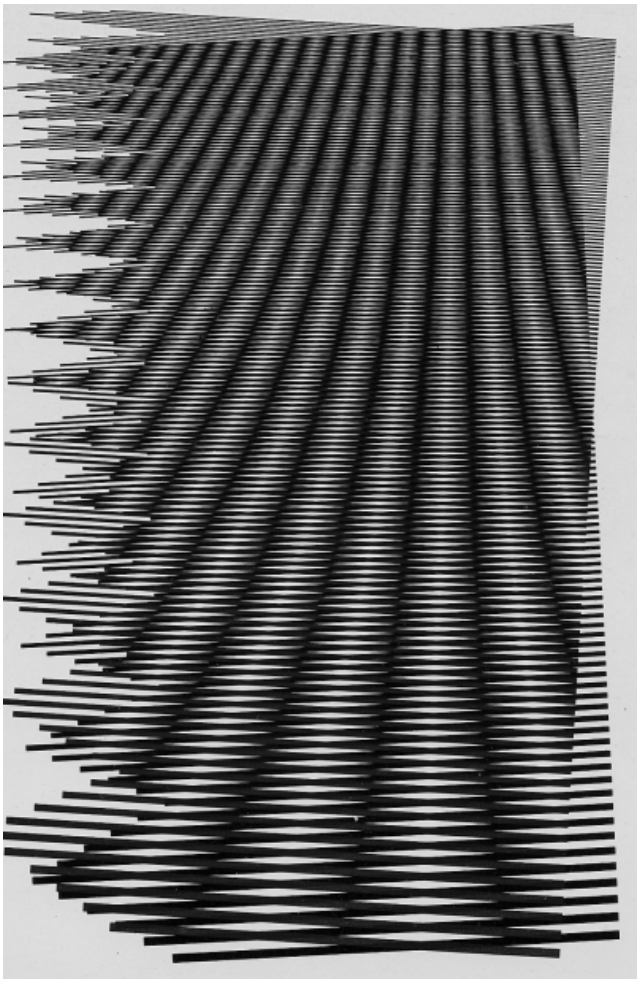

Fig. 14.8 Moiré pattern for two waves whose direction of phase propagation is slightly different. As the two images are moved vertically relative to one another the positive interference bands move, in this case to the left or right. This shows that energy propagation, corresponding to the movement of bands of positive intereference, occurs in a direction different from the phase propagation which is vertical in this picture. The phase speed of Rossby waves varies with both wavelength and direction of propagation, and the energy moves in a direction 2μ, where the direction of the wavevector is μ, measured from East. (Eqn.(14.19) .

14.6 *Summary of barotropic Rossby wave properties.* The waves are:

- dispersive (the phase speed varies with wavelength), although waves much longer than the ¤Rossby Radius, λ_{BT}, are non-dispersive, $\sigma \cong -\beta k\lambda^2$. For waves much shorter than λ_{BT}, the free surface is effectively rigid, and the wave equation becomes

$$\nabla^2\psi_t + \beta\psi_x = 0$$

Here we have used the streamfunction ψ as dependent variable, recalling that in the quasi-geostrophic, barotropic theory, the free surface height, pressure perturbation, and streamfunction are all proportional to one another, $f_0\psi = g\eta = p'/\rho$;

- anisotropic (the phase speed and frequency vary with direction of propagation, even for a fixed wavelength).

- have wavecrests with westward movement of phase along latitude circles, $\sigma/k < 0$. This also describes the topographic waves calculate above, if the topography slopes upward to the north; adjust accordingly for other orientations of the slope, so that the wavecrests always move with shallower water to their right. The gradient of f/h is the generalized β-effect for topographic Rossby waves.
- energy propagation, with group velocity

$$\vec{c}_g = (\frac{\partial \sigma}{\partial k}, \frac{\partial \sigma}{\partial l})$$

is directed at twice the angle of the wavevector, as measured with respect to East, and its magnitude is equal to the westward phase speed, $\beta / |\vec{k}|^2$. The group velocity, $\vec{c}_g$, is the gradient of the surface σ(k,l), hence is perpendicular to the contours of constant frequency, pointing toward higher values of σ;

- they are 'vorticity waves' which are nearly non-divergent (the horizontal divergence, u_x+v_y is small,

  O(Ro) compared with vorticity $\zeta = v_x - u_y$);
- they are nearly geostrophic, $u_t << fv$ or $g\eta_x$;
- their frequency increases with wavelength;
- the vertical vorticity, $\zeta = (g/f)\nabla^2\eta$;
- the horizontal velocity is related to the free surface slope according to (5.1),

$$u = g\frac{-f\eta_y + i\sigma\eta_x}{f^2 - \sigma^2}; v = g\frac{f\eta_x + i\sigma\eta_y}{f^2 - \sigma^2}$$

The high- and low-frequency limits of these expressions speak for themselves.

- the ratio of potential energy, ½ $g\eta^2$, to horizontal kinetic energy, ½ $\rho(u^2 + v^2)$, varies as L^2/λ_T^2, L being the horizontal length scale.

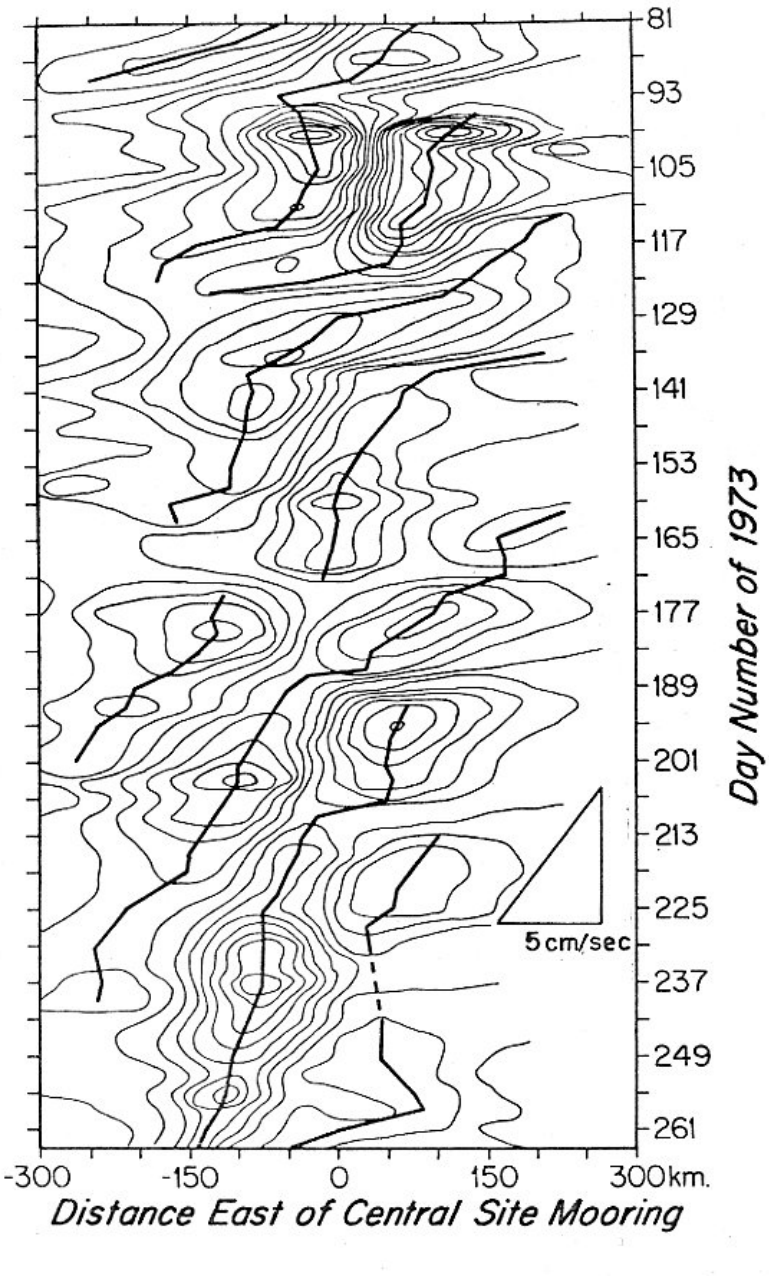

Fig. 14.9. Space-time ('Hoevmueller') plot of meridional velocity against longitude and time, from the MODE-73 experiment in the western Atlantic near 30N. This is possibly the first sighting of Rossby waves in the ocean. Time progresses downward, and the phase of the 100km scale eddies moves westward at about 5 cm sec^{-1}. Freeland *et al.* (1975).

14.7 *Reflection of a Rossby wave at a north-south boundary.* If a meridional boundary, a straight, vertical wall, lies at x = 0, then a Rossby wave traveling westward toward it will be reflected. The boundary condition $u=-\partial\psi/\partial y=0$ at x=0 is satisfied by adding a reflected wave with just the right k, l and σ. Write

$$\psi = A\exp(ikx+ily-i\sigma t)+A'\exp(ik'x+il'y-i\sigma' t)$$

where the primes indicate the reflected wave. We require at x=0

$$ilA(\exp(ily - i\sigma t) = -il'A'(\exp(il'y - i\sigma' t)$$

For this to be satisfied at all times and all y, we must have l=l', σ=σ', A=-A'. This leaves us the two values for k and k',

$$k = -\beta / 2\sigma \pm (\beta^2 / 4\sigma^2 - l^2 - \lambda^{-2})^{1/2}$$

found by drawing a horizontal line through the wavenumber curve for this frequency and y-wavenumber. The incident wave has westward group velocity, and is longer than the reflected wave (|k|<|k'|). This explains the patterns seen in numerical models of Rossby wave propagation, long waves rapidly propagating west to the boundary and short waves propagating back eastward, much more slowly. Now the amplitudes of the streamfunction for incident and reflected waves are the same, but the velocity is proportional to the gradient of ψ or η, and hence the reflected wave will be more energetic, by a factor $(k'/k)^2$. This works so as to conserve energy flux, which is energy density multiplied by group velocity.

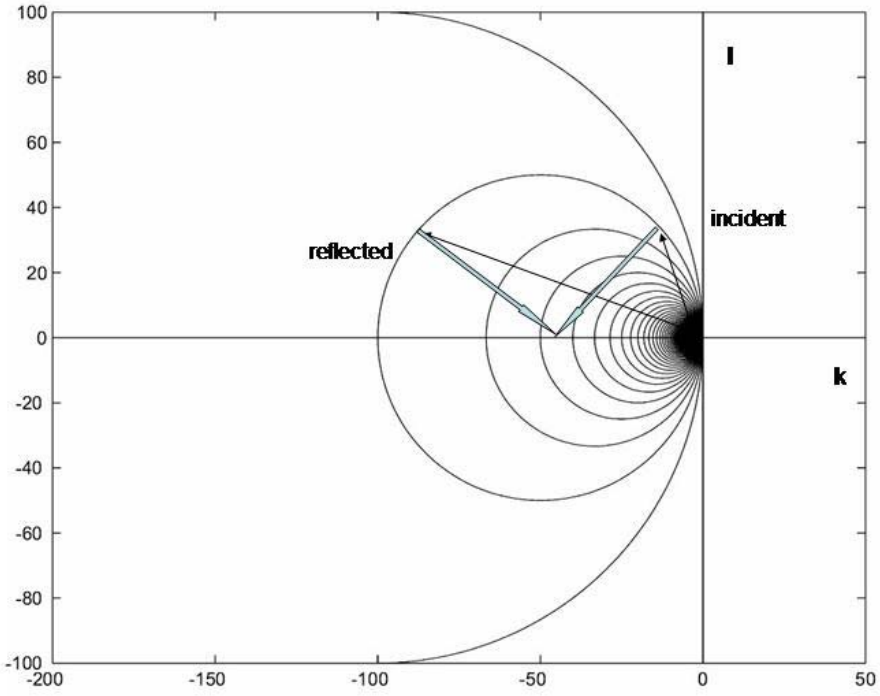

Figure 14.10 Incident and reflected Rossby waves at a north-south rigid boundary; wavevectors are thin arrows and corresponding group velocities are filled arrows. The group velocity reflects symmetrically about the normal to the boundary, yet the reflected wavevector is longer than the incident wavevector, so that the reflected wavelengths are shorter.

Because frictional/turbulent damping of Rossby waves can be important, the slower propagating waves will be affected most strongly. This means that energy will propagate rapidly across the ocean to the western boundary and reflect, yet will dissipate before

propagating far from the boundary. Energy 'piles up' in small-scale currents and dissipates near western boundaries of oceans. Indeed, the level of eddy kinetic energy is observed to be higher in these regions than in mid-ocean.

A generalization of the effect of boundaries on β-plane fluid. When one encounters a strong prediction of theory like this one, there is the temptation to see if it may be more general. Linear wave theory and its limits are examined later, in Chap. 17. As a precursor of these ideas, consider the conservation principle for enstrophy (enstrophy, introduced in Chap. 13, is squared vertical vorticity, or potential vorticity depending on circumstances). For a barotropic β-plane fluid surrounded by rigid boundaries, the inviscid PV equation is

$$\frac{D(\zeta + f)}{Dt} = 0$$

$$\nabla^2\psi_t + J(\psi, \nabla^2\psi) + \beta\psi_x = 0$$

with the free-slip condition,

$$\nabla\psi \times \hat{n} = 0$$

applied on the boundary, C, where the outward normal unit vector is $\hat{n}$. Multiply this equation by $\nabla^2\psi$ and integrate throughout the fluid, over the area A, with the result

$$\frac{d}{dt}\iint_A \tfrac{1}{2}|\nabla^2\psi|^2 dx\,dy = -\oint_C KE \sin\alpha_B ds \qquad (14.20)$$

where KE = ½ $|\nabla\psi|^2$ is the kinetic energy and α_B is the angle of the boundary, with respect to East. The righthand side of the result follows from integrating $\psi_x\nabla^2\psi$ by parts and applying the free-slip boundary condition. Enstrophy has smaller spatial scale than energy, for motions with a broad spectrum (the enstrophy spectrum is the energy spectrum multiplied by (k^2+l^2), equivalent to a high-pass filter in wavenumber space). Eqn. (14.20) says that even though the total energy in fluid is constant (absent dissipation and forcing), energy in the fluid at a boundary lying to its east will decrease the total enstrophy, while energy in fluid at a boundary lying to the west will increase the enstrophy. This is true for turbulent motions, circulation and waves and represents a generalization of the Rossby wave reflection property discussed just above. The ratio of total energy/total enstrophy is a length squared, an average measure of length scale of the currents and this changes with time. The result is also a precursor to the existence of narrow, intense western boundary currents, to be discussed in Chap. 15.

14.8 *Rossby waves generated by a point source of pv: Green's function.* A single, plane wave is an elegant solution of the equations. As remarked in Section I of this book, the dispersion relation sums up the physics of the problem, and allows spatial structure of an initial pattern of flow (determined by its amplitude for different wave-vectors, $\vec{k}$) to be calculated into the future (with the time-dependence following from the unique frequency, ω, associated with each $\vec{k}$). In *dispersive* wave systems, a compact forcing region sends

out waves which sort into these Fourier components as we saw with Kelvin's solution, the 'impulse response' for a gravity wave field produced by an initial disturbance of very small spatial extent.

That 'impulse response' is a complementary approach to the consideration of individual plane waves: the field of waves produced by a small region of forcing, so small that it is represented by Dirac's delta function, say $\delta(\vec{x})$. The delta function is simply a limiting case of a tall, narrow function that preserves the volume beneath it as it is made ever narrower. A frequent choice is the Gaussian function,

$$\delta(r) = \lim_{a \to 0} (1/\pi a^2) \exp(-(r/a)^2)$$

Limiting sequences of functions of this kind are sometimes known as 'generalized functions'; they play a fundamental role in making Fourier transform theory, and hence wave theory, more rigorous (*e.g.*, Lighthill, 1958).

For convenience we suppose the forcing is at the origin, $\vec{x}$=0. The forcing can also be impulsive in time, and 'explosive' $\delta(\vec{x})\delta(t)$, or it can be oscillatory with a single frequency, $\delta(\vec{x})\exp(-i\omega_0 t)$. Waves propagate outward from the origin, filling the space until they encounter a boundary or are damped by friction. Such solutions are also known as 'Green's functions', and there is considerable mathematical development associated with them. In geophysics, where one is interested in the first and largest waves related to an earthquake or tsunami, they are sometimes called 'propagators'. In ocean/atmosphere fluids such solutions have been thoroughly described by Dickinson (1966).

We want to solve the forced wave equation,

$$\nabla^2 \psi_t + \beta \psi_x = F(\vec{x}) \exp(-i\sigma_0 t)$$

for the choice of forcing function

$$F = \delta(r) .$$

To do this, notice that a change of dependent variable converts the left-hand side into a Helmholtz equation: let

$$\psi = \Phi(x, y) \exp(-i\beta x / 2\sigma_0 - i\sigma_0)t)$$

Substitution gives immediately

$$\nabla^2 \Phi + \kappa^2 \Phi = \delta(\vec{x})$$

$$\kappa \equiv \beta / 2\sigma_0$$

The equation has been rendered isotropic (independent of direction), and essentially the same as for waves on a membrane excited by an oscillating, impulsive force. Exploiting this isotropy, we look for solutions depending on radial coordinate, $\Phi(r)$ only, and we write the equation in cylindrical polar coordinates (r,θ) :

$$\Phi_{rr} + \frac{1}{r}\Phi_r + \kappa^2\Phi = \delta(r)$$

This is Bessel's equation, one of the classic equations of mathematical physics. It is here in its isotropic form; more generally Bessel's equation allows for structure in the azimuthal, θ- direction. It arises in many problems of waves with cylindrical geometry (this choice may be dictated by either the shape of the boundaries or the forcing effect). The solutions are the sine-waves of cylindrical geometry and like standing and traveling sine-waves they come in a family. $J_0(r)$, $Y_0(r)$, $H_0^{(1)}(r)$, $H_0^{(2)}(r)$, correspond respectively to the more familiar cos(r), sin(r), exp(-ir), exp(+ir) wave solutions in Cartesian coordinates. How is the choice made? As usual, by applying boundary conditions, in this case what is known as the *radiation condition,* stating that the waves must carry energy outward, away from the wave-source, at large r (we could contrive a wave-maker at large r that would send waves inward, we could be in a circular ocean basin whose coast would reflect the waves). Consulting Abramowitz and Stegun (1970) or another source of formulae for mathematical functions, we find that at large radius, Bessel functions have the following asymptotic forms for $kr \to \infty$:

$$J_0(kr) \sim (\pi/kr)^{1/2}\cos(kr - \tfrac{1}{4}\pi)$$
$$Y_0(kr) \sim (\pi/kr)^{1/2}\sin(kr - \tfrac{1}{4}\pi)$$
$$H_0^{(1)}(kr) \sim (\pi/kr)^{1/2}\exp(i(kr - \tfrac{1}{4}\pi))$$
$$H_0^{(2)}(kr) \sim (\pi/kr)^{1/2}\exp(-i(kr - \tfrac{1}{4}\pi))$$

showing a simple relationship with ordinary sines and cosines; the $r^{-1/2}$ decrease in amplitude with increasing radius follows from the spreading of wave energy in space, far from the origin. The right solution is now apparent: referring to Fig. 14.3, notice that the projection of its group velocity on the wave-vector is always negative, so that a wave propagating energy outward will have phase moving inward along the radial direction. Inward phase propagation occurs only for the choice

$$H_0^{(2)}(\kappa r)$$

and hence the total solution for this wave problem is

$$\psi = \exp(-i\kappa x - i\sigma t)H_0^{(2)}(\kappa r)\,. \qquad (14.21)$$

At large distance from the origin (relative to the wavelength), the Green function becomes

$$\psi = \sqrt{\pi/2\kappa r}\exp(-i\kappa(x+r) - i\sigma t) \qquad (14.22)$$

Curves of constant phase, κC, are

$$x + r = C$$
$$r(1+\cos\theta) = C$$
$$y^2 = C(C - 2x)$$

which are three ways of writing a set of parabolas whose foci are $x = \frac{3}{8}C$ (the value of C selects which wave-crest we are watching). An animation of the wave-field (Fig. 14.11) shows the wavecrests to sweep westward while collapsing on the negative x-axis. The phase of each wave-packet making up the pattern has a westward component. This solution makes a good case for the value of theory. We could have stopped after deriving the group velocity, and done numerical simulations of Green's functions by computer. But in doing so we might have missed the simple structure, the parabolic wave crests, and unless we did many such simulations, missed the importance of the length-scale parameter $\kappa^{-1} \equiv (\beta/\sigma_0)^{-1}$. The study of classical functions like Bessel functions and the corresponding functions arising in spherical geometry blossomed in the 19th Century, long before computers were available. They helped provide a firm basis in theory for physical dynamics in natural science and technology, where differential equations are often the governing theory. Using Matlab, Mathematica or other mathematical software one can explore the functions very easily, animate the wave-field. In particular, the simple asymptotic forms for small and large argument overlap nicely, allowing wave theory to proceed more easily.

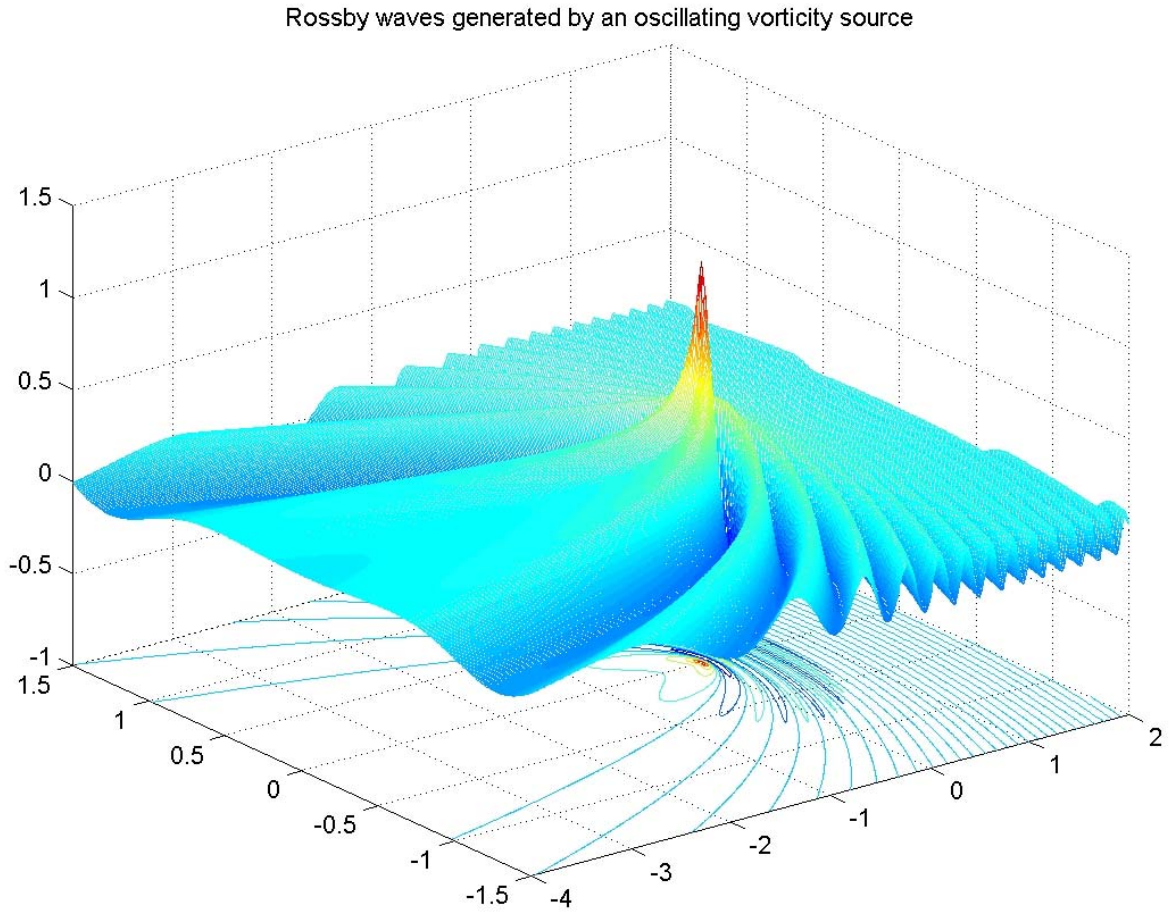

Fig. 14.11 Rossby wave pattern, Eqn. (14.21), created by an oscillating, small disturbance at the origin. Plotted is the pressure, or free-surface elevation η, or streamfunction ψ, at a particular time, as seen from the southwest (negative y, negative x). The parabolic wave-crests (see as contours on the base plane) sweep westward with time, closing in on the negative x-axis.

A meridional boundary can be included in this theory, for example a north-south wall lying to the west of the forcing point. The method of images is a technique of classical mathematical physics, where one uses ideas of symmetry to add a boundary to a flow field. Here, if the oscillatory wave source is placed at the point (A,0) we place an identical 'image' source of Rossby waves at the point (-A, 0). Adjusting the phase properly will create a line along which the zonal velocity, u, vanishes at all time. Now, the 'twist' is that our Rossby-wave Green function is anisotropic, so that the image source produces much shorter Rossby waves in the vicinity of the wall, those that radiate eastward from x = -a, than does the direct source. And, the amplitude of the currents, spatial derivatives of ψ, from the image source near x = 0 is much greater than that of the direct source because of this contrast in wavelength. This simple construction provides yet another generalization of the reflection properties of Rossby waves at a rigid lateral boundary.

Energy conservation can be verified for this solution. A wave packet, which is a plane wave tapered off to nothing after many wavelengths, move with the group velocity and their energy must move with them (because they are isolated concentrations of energy surrounded by emptiness). As described in Sec. I, the product of energy density $\mathcal{E}$ and group velocity $\vec{c}_g$ equals energy flux,

$$\vec{F}_E = \mathcal{E}\vec{c}_g .$$

The energy equation

$$\mathcal{E}_t + \nabla \bullet (\mathcal{E}\vec{c}_g) = 0$$

for a 'statisitically steady' wavefield, whose amplitude is not changing with time, says that the integral of the energy flux component normal to a bounding surface, over the entire surface, should equal the constant rate of supplying energy to the wavefield at the origin,

$$\int_0^{2\pi} \vec{F} \bullet \hat{r} \; r\, d\theta = const.$$

where $\hat{r}$ is a unit vector directed along the radius. Here, with negligible contribution of the free-surface potential energy, the energy density is $\frac{1}{2}|\nabla\psi|^2$ per unit mass. In the far field, κr >> 1, the gradient of ψ is dominated by the wavy exponential, and not the gradual variation in amplitude. Differentiating the exponential factor in Eqn. (14.22)

$$\mathcal{E} = \tfrac{1}{2}\rho|\nabla\psi|^2 = \tfrac{1}{2}\rho|\vec{k}|^2|\psi|^2 + O(\kappa r)^2 = \tfrac{1}{2}\rho(\pi/\kappa r)2\kappa^2(1+\cos\theta)$$

Energy propagates directly outward from the source, and therefore the group velocity points radially outward everywhere. Its magnitude $|\vec{c}_g| = \sigma/k = \beta/|\vec{k}|^2$ varies inversely with wavenumber squared, which makes the product $\vec{F}_E = \mathcal{E}\vec{c}_g$ isotropic! Despite all of the strange anisotropies of Rossby waves, energy radiation from an oscillating point source is independent of direction. The energy flux total outward is just $\frac{1}{2}\rho\beta\pi/\kappa r = \pi\rho\sigma_0/r$, and its integral over all directions 2πr times this, or $2\pi^2\rho\sigma_0$, independent of r, so that energy is conserved.

For a wave-maker at an arbitrary postion $\vec{x}'$ we write the Green function symbolically as $G(\vec{x},\vec{x}')$. This allows us to express the wave field for a forcing function of arbitrary shape and size, for in this self-adjoint equation it may be shown that the solution of Eqn. (14.21) is

$$\psi = \iint F(\vec{x}')G(\vec{x},\vec{x}')d\vec{x}' .$$

where the integration is over the entire fluid. This is the power of Green's function, that it gives the solution for waves forced by a wave-maker of complicated form, in terms of wave solution for a single, small isolated wavemaker. In words, ψ is the *convolution*

integral of F and G. The wave equation is linear, and here we are superposing an infinity of Green-function wave patterns, each generated at a different location by the forcing function with amplitude given by $F(\vec{x})$. Valuable insight follows: since the delta function is only infinitesimally wide, we want to know what a forcing effect of finite size will produce. The theory of Fourier transforms (Appendix 4) tells us that the transforms of $\psi(\vec{x}), F(\vec{x}), G(\vec{x})$ call them $\tilde{\psi}(\vec{k}), \tilde{F}(\vec{k}), \tilde{G}(\vec{k})$, are related as a simple product:

$$\tilde{\psi}(k,l) = \tilde{F}(k,l)\tilde{G}(k,l)\,. \qquad (14.23)$$

We can now visualize the Rossby wave field generated by a forcing region of finite size, by overlaying the two transforms on the wavenumber plane. Because it involves the product of transforms in Eqn. (14.23), the solution only has substantial amplitude for wavenumbers where both $\tilde{F}$ and $\tilde{G}$ are non-zero. As we learn from the example of the Gaussian bell-curve (also see Appendix 4), the Fourier transform of a compact function with length-scale L is concentrated at wavenumbers less than or equal to 1/L. Because the locus of Rossby wavenumbers for the frequency σ_0 extends only to wavenumbers of magnitude $\leq \beta/\sigma_0$. If, for example, Rossby waves are generated by forcing with an oscillating wind of horizontal scale L, decreasing the *frequency σ_0, so that $\sigma_0/\beta L << 1$, will pick out predominantly waves west of the forcing region, and these waves will resemble slowly oscillating zonal currents.* This is illustrated in Fig. 14.¤.

Transient Rossby waves occur when forcing is suddenly switched on, or otherwise radiating from an initial condition without further forcing. The wave pattern then involves a spectrum of frequencies, rather than the single frequency in Fig. 14.11. An initial condition in the form of a circular eddy evolves as shown in Fig. 14.12: a 'weak' eddy 'explodes' into Rossby waves (whereas an eddy with greater velocity will remain coherent longer, resisting Rossby-wave radiation).

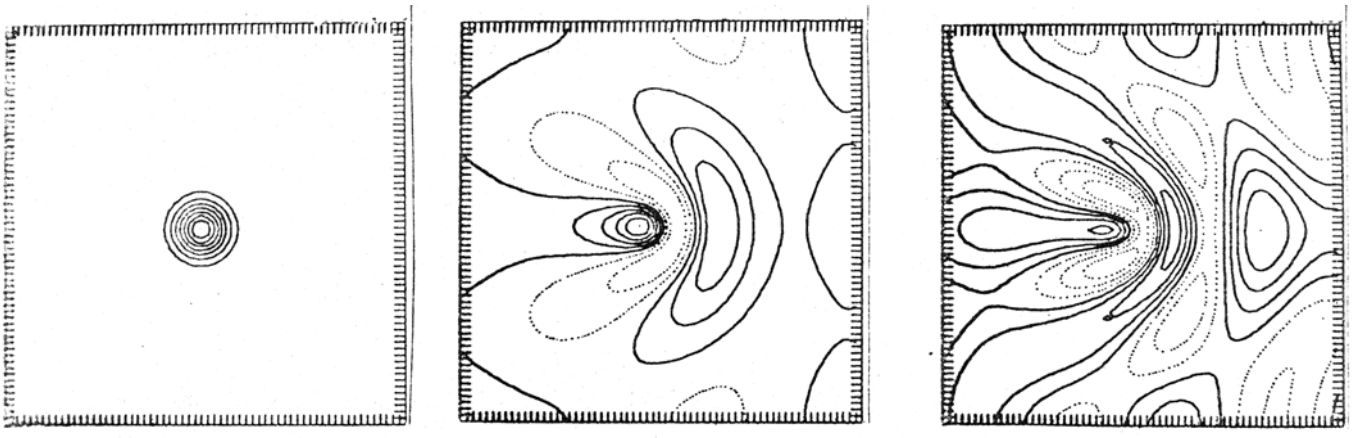

Fig. 14.12 An initially specified velocity field in the form of a circular eddy radiates Rossby waves (barotropic, β-plane with periodic boundary conditions, so that westward radiation re-enters the domain from the east).

Numerical simulations of this kind are readily carried out, even on a lap-top computer. Some sample codes to achieve this are included in Appendix ¤.

Rossby waves can be produced in the laboratory, using variations in depth to provide a large-scale PV gradient analogous to the β-effect. The simplest method is to let the paraboloidal free surface of a rapidly spun fluid in a cylinder provide essentially a polar β-plane. With excitation sinusoidal in time, at a point in space, the field is dominated (Fig. 14.13) by eastward propagating short Rossby waves, when visualized by the movement of rings of dye. When instead the velocity field is observed using fine, floating metallic particles, the long westward-propagating waves are visible, with wave-crests that spiral in toward the Pole. Animations show the 'elasticity' of the fluid provided by PV gradients, with Jello® like oscillations communicated throughout the domain (Rhines, 2003b), and also with the elasticity inhibiting mixing of the 'ozone hole' at the Pole.

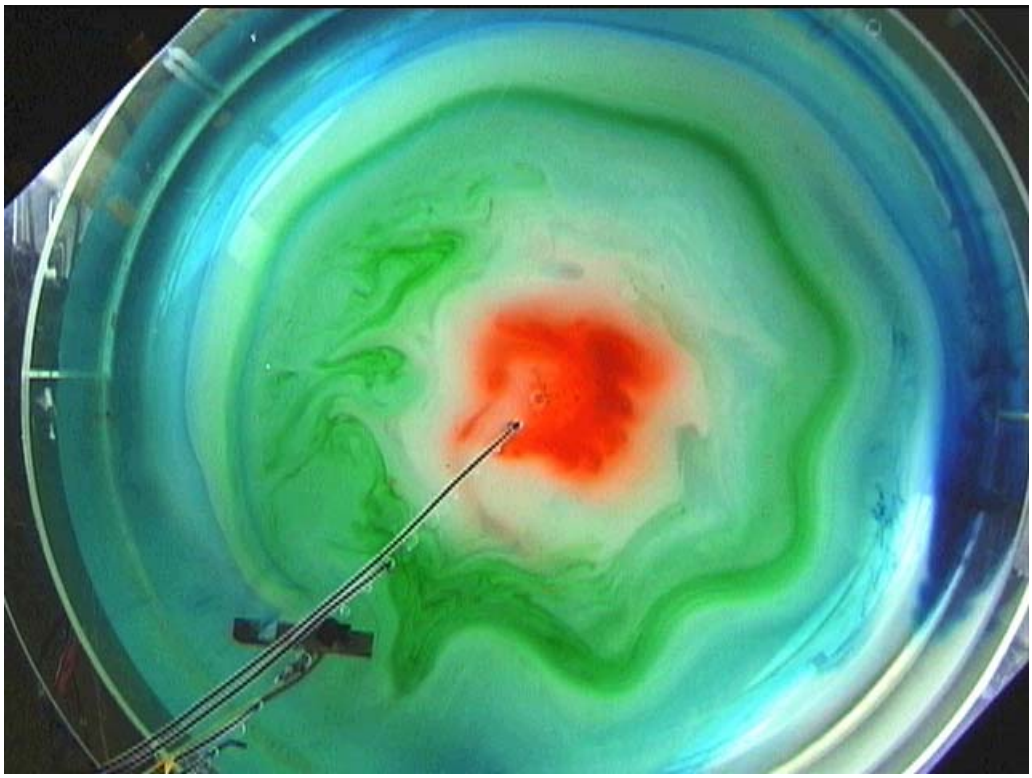

Figure 14.13. Rossby waves in the laboratory, as if viewed by a satellite above the North Pole. The wave source is at the lower left, and oscillating body. There is no pre-existing circulation, but the waves induce easterly flow at most latitudes, and westerly flow at the latitudes near the forcing (as seen in the dye

drawn into circles). At the North Pole, the red dye remains unmixed by the strong wave activity. (Rhines (2003), Geophysical Fluid Dynamics Laboratory, University of Washington.)

14.9 *Rossby waves in a zonal current.* In the Southern Ocean the Antarctic Circumpolar Current (the greatest of ocean currents, by many measures) flows eastward beneath the strong zonal winds. As it flows above seafloor ridges and through gaps like the Drake Passage, Rossby waves are excited; they tend to be *standing waves* with zero phase speed, a meandering of the current. In the atmosphere one is almost always dealing with waves on top of mean winds. As a basic model, suppose there is a strong zonal flow, u = U, a constant. We then must retain the advective term $U\partial\zeta/\partial x$ in the vorticity equation. This adds a term to Eqn. (14.17) which becomes

$$\nabla^2\psi_t + U\nabla^2\psi_x + \beta\psi_x = 0$$

Substituting the usual plane wave solution we find the modified dispersion relation,

$$\sigma - Uk = -\beta k/(k^2 + l^2)$$

where we have temporarily neglected the term $1/\lambda^2$, appropriate to waves shorter than the Rossby deformation radius, $L << \lambda$.

Consider standing waves with zero frequency (the waves have a non-zero frequency for an observer moving with the mean flow, given by the usual dispersion relation). The wave equation becomes closely related to Helmholtz's equation:

$$\frac{\partial}{\partial x}(\nabla^2\psi + \frac{\beta}{U}\psi) = 0 \qquad (14.24)$$

with dispersion relation

$$Uk = \beta k/(k^2 + l^2)$$

which has two solutions,

$$k = 0; \quad k^2 + l^2 = \beta/U\ .$$

as shown in Fig. 14.13. The second solution is simply a circle in wavenumber space and exists only for U>0; because of their intrinsic westward phase propagation relative to the fluid, Rossby waves can stand still on an eastward current. All waves generated in this way have the same wavelength, $2\pi(U/\beta)^{1/2}$. The group velocity vectors are normal to the circle, as usual, yet they point always with a component downstream (eastward). It is easy to sketch the wave pattern generated by a localized, small source of waves near the origin, x=y=0. The isotropic nature of the wavenumber circle in Fig. 14.13 determines that the wavecrests are also circular. With the group velocity directions as above, the waves appear only downstream, so they have *semi*-circular wave-crests. It is a good exercise to construct these results graphically by adding the intrinsic group velocity to a uniform eastward velocity (U,0). In doing so one finds that the magnitude of the group velocity in this new situation varies as $\cos(\theta)$, and hence if the wave source is switched on at some

initial time, the Rossby wave wake will fill out in a circle whose radius increases with time. In particular the region filled with waves expands downstream in advance of the current, at just twice the velocity (U,0) of the mean flow. {A simple graphical procedure for constructing the wave-crest pattern on the (x,y) plane from the locus of possible wavevectors on the (k,l) plane is described by Lighthill (1968): see Appendix ¤}.

The figure 14.14 shows the exact linear solution, McCartney (1975) where the waves are generated by flow over an idealized mountain (dashed circle). The shape of the wave-crests carries with it information about the transport of momentum by the wave, which will be discussed in Chap. 17.

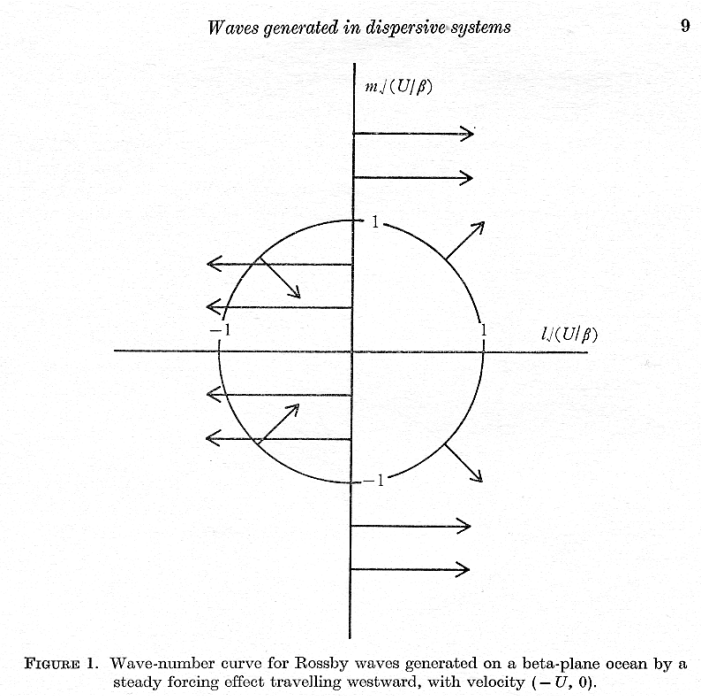

FIGURE 1. Wave-number curve for Rossby waves generated on a beta-plane ocean by a steady forcing effect travelling westward, with velocity $(-U, 0)$.

Figure 14.13 Locus of wavenumbers for barotropic Rossby waves, generated either by a uniform eastward flow over a topographic mountain, or by a forcing effect that moves steadily westward over initially still fluid.

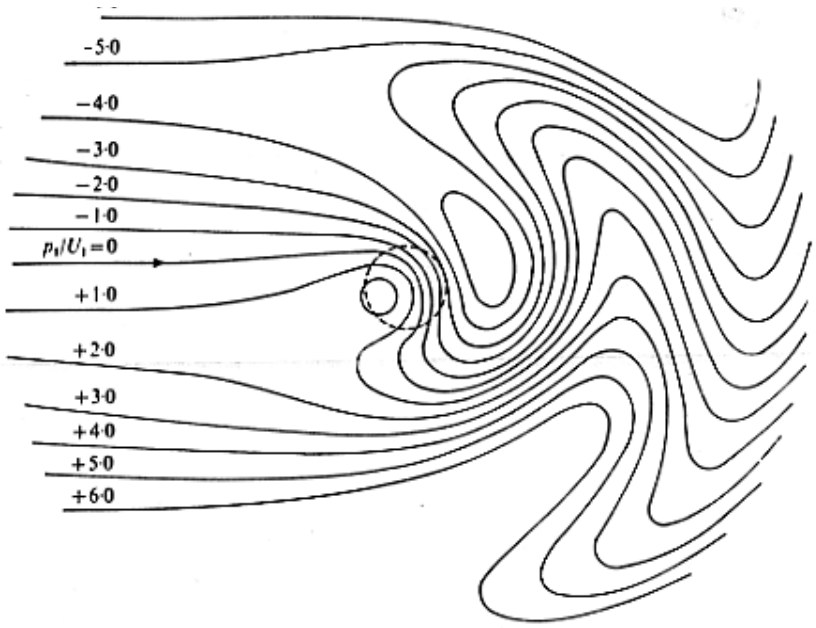

Figure 14.14 Rossby waves on an eastward current generated by a small 'mountain' (a right circular cylinder at the origin); from McCartney (1975). This is an exact linear-wave solution of the steady PV equation. The semi-circular wavecrests predicted by theory can be seen in the lee of the mountain. Note that cyclone downstream of the mountain; its low pressure, compared with the flow upstream, exerts a wave-drag on the topography which is expressed as a flux of zonal momentum in the wave-field.

The first of the two solutions of the dispersion relation is quite remarkable. It looks as if it should be thrown away. Yet, k=0, if understood as a limiting case where k << l, is very much a Rossby wave, with wave-crests lying nearly east-west. The frequency relative to the fluid nearly vanishes for such a wave, yet look at its group velocity: it is as large as it can be, and in a frame of reference moving with the fluid, the group velocity is westward. The direction of the group velocity in the frame of reference fixed with the mountain, in this limit is east or west. The sign depends on whether the intrinsic group velocity (relative to the fluid) is greater or less than U. Since the intrinsic group velocity defined in this way is $(-\beta/l^2, 0)$ for k=0, then the total group velocity in the frame of reference of the mountain is $(U-\beta/l^2,0)$. The sign change occurs at $l^2 = \beta/U$, at the radius of the circle of wavenumbers for the 2d solution. The longer waves propagate upstream and act to block the flow; shorter waves are carried downstream; see Lighthill (1978). The straightness of the l-axis which 'generates' the blocking waves tells us that the group velocity does not diverge (always points due west or due east); this says that the blocking pattern propagates far upstream and downstream with little reduction in strength.

14.10 *Baroclinic Rossby wave modes in a stratified ocean.* The study of long baroclinic waves is of interest to both time-dependent ocean currents and the mean

circulation. As we have argued earlier, waves are the forerunners that set up circulation, in initial-value problems (as in switching on the winds) and in course of seasonal and longer-period variability of the forcing effects. Density stratification allows Rossby waves to propagate in all three spatial dimensions, just as it does with internal gravity waves. In fact we have already done much of the work needed to study the baroclinic waves, because of the *separable* nature of the β-plane equations with uniform depth and horizontally uniform stratification (under the traditional approximation, neglecting the horizontal component of Earth's rotation vector). This means that the equation for the vertical structure of Rossby waves is the same as that for internal gravity waves without rotation (subject only to possible differences in upper and lower boundary condition).

For the oceanic case we make the Boussinesq approximation, because the scale height of the density field is so large compared with the depth of the ocean. The β-plane approximation is accurate to order L/a in middle latitudes, and to order $(L/a)^2$ in the Equatorial zone. The mid-latitude synoptic-scale potential vorticity equation (13.42) is

$$\frac{D_g q}{Dt} = F - D$$

$$q = \nabla^2\psi - \frac{\partial}{\partial z}\left(\frac{f_0^2}{N^2}\frac{\partial \psi}{\partial z}\right) + \beta(y - y_0) \qquad (14.25)$$

$$\frac{D_g \bullet}{Dt} = \frac{\partial \bullet}{\partial t} + J(\psi, \bullet)$$

The Boussinesq approximation is also used here, eliminating applications involving 'tall' atmospheric disturbances. The familiar relative vorticity, 'stretching' and planetary vorticity components of the PV are all active to some degree in baroclinic Rossby waves but scale analysis of q shows that for horizontal length scales, L, greater than the Rossby deformation radius, λ, the relative vorticity contribution becomes small. The symbolic forcing term F and dissipation D will be developed later.

The wave equation follows from the neglect of the nonlinear terms in (14.25):

$$\nabla^2\psi_t + (\frac{f_0^2}{N^2}\psi_z)_z + \beta\psi_x = 0 \qquad (14.26)$$

Disregarding the top and bottom boundaries for the moment, we note that the coefficient of the middle term in the equation is a function of z only, and therefore there are solutions in which the vertical dependence is separated out, having the form

$$\psi = \Xi(z)\hat{\psi}(x, y, t) \qquad (14.27)$$

The simplest case occurs with uniform density stratification, N = const., for which the substitution of a three-dimensional plane wave, $\psi = \mathrm{Re}(\exp(i(kx + ly + mz - \sigma t)))$, yields the dispersion relation

$$\sigma = \frac{-\beta k}{k^2 + l^2 + f_0^2 m^2 / N^2} \qquad (14.28)$$

Here we continue use of the term 'Rossby deformation radius' to mark the horizontal scales at which potential energy and kinetic energy are comparable in size, we have a set of Rossby radii which depend on vertical scale of the waves,

$$\lambda_{BC} = \frac{N}{f_0 m}.$$

For more complicated stratification profiles, the more general form (14.27) is substituted in Eqn. (14.26) and divide by $\Xi\psi$; just as we found with internal gravity waves the equation contains some terms dependent on z only, and others dependent on (x,y,t) only: each of the two groups must vanish separately or at most be equal to a constant A:

$$\nabla^2 \hat{\psi}_t + \beta \hat{\psi}_x + A^2 \hat{\psi} = 0$$

$$\left(\frac{f_0^2}{N^2} \Xi_z \right)_z - A^2 \Xi = 0$$

This allows us to solve for the vertical structure, $\Xi(z)$, once and for all. Equation and boundary conditions together form an eigenvalue problem for A. The Rossby deformation radius emerges from this eigenvalue problem. The boundary conditions are

$$\psi_z = 0 \text{ at } z = 0, -H$$

Strictly speaking, these follow from the vanishing of vertical velocity, w, at the boundaries (ψ_z is proportional to density perturbation ρ' which also vanishes, because in this situation ρ' can only arise from vertical movement of the basic stratification). The fact that the surface is free, and moves slightly, adds a slight error proportional to the amplitude of the wave. For density stratification typical of the Earth's oceans, this is a very small error.

For the choice above, uniform density stratification, the vertical modes with boundary condition of vanishing vertical velocity at top and bottom are

$$\xi = \cos(mz), \;\; m = n\pi / H, \;\; n = 1, 2, 3....$$

representing pairs of upward and downward traveling waves that form a standing mode with stationary horizontal nodes. The resulting equation for the horizontal structure of the wave is just Eqn. (14.26) and plane waves have the form

$$\psi = \cos(mz) \exp(ikx + ily - i\sigma t)$$

with the dispersion relation (14.28). The oceanic baroclinic Rossby wave dispersion relation has just the same form as the barotropic wave equation with a free surface, and as in that case, waves shorter than λ_{BC} have dominantly kinetic energy while waves longer than λ_{BC} are dominated by potential energy associated with vertical displacement of the isentropic surfaces. The 'gravest' Rossby radius, for the lowest baroclinic mode n=1, ($\lambda_{BC} = NH/f_0\pi$ for uniform N) is a key descriptive parameter of the water column, and the

complete set of Rossby radii are conveniently expressed as c_n/f_0, where c_n is the horizontal phase speed of long, nearly hydrostatic internal waves in the n^{th} vertical mode.

For oceanic scaling, baroclinic Rossby waves propagate very slowly at mid- to high latitude, though their phase speed increases substantially near the Equator. With typical ocean stratification the first vertical mode (n = 1) has phase speed of 2 to 5 cm sec^{-1}, so that at 30^0N latitude it takes of order 10 years to cross the Atlantic ocean. Yet the waves are important in controlling the structure of the general circulation, which is the subject of Chap. 15.

Long, linear baroclinic Rossby waves are non-dispersive. They simply propagate westward without change of form. This is the limit $L >> \lambda_{BC}$, for which the dispersion relation becomes

$$\sigma = -\frac{\beta \lambda_{BC}^2 k}{m^2 H^2}$$

so that the 'gravest' mode, n = 1, or $m=\pi/H$, moves westward with speed $\beta\lambda_{BC}^2/\pi^2$.

Satellite altimetery exhibits a rich field of westward propagating waves, as seen, not in the displacement of constant-density surfaces, but in much smaller displacement of the sea surface. The satellite altimeter can detect sea-surface heights with relative accuracy of order 1 cm. at these scales (a remarkable engineering accomplishment, in view of the large gravity waves on the surface). We might expect these to be primarily barotropic Rossby waves, yet the greater energy present in baroclinic modes makes them stand out, even in the SSH field. Geostrophic balance for the velocity field shows that there must be such ups and downs of the sea surface, for hydrostatic balance to provide the lateral pressure gradients: typically, an eddy with height anomaly of 5 cm and lateral scale 500km has a geostrophic surface current of $g\delta\eta/fL \sim 1$ cm sec^{-1} at middle latitude. Animations of the global SSH field, available from many sources on the Web, exhibit a rich parade of propagation, with striking westward propagation of features greater than 100km in width, downstream movement of eddies in boundary currents, and rapid Kelvin- and Rossby waves along the Equator. Chelton and Schlax (1996) plot global maps of the sea-surface height anomaly (Fig. 14.15), and time-longitude structure of the sea-surface in the Pacific (Fig. 14.16). After spatial filtering to eliminate mesoscale eddies, the figure shows westward propagation, with speeds that decrease with latitude as expected. In a striking affirmation of the non-dispersive limit of the theory, a single dominant speed occurs at each latitude. These are related to the n = 1 mode; the concentration of the density stratification in the upper ocean also concentrates the first baroclinic mode there, rather as in layered ocean model with a thin upper layer.

The variation of phase speed with latitude is shown in Fig. 14.17, for the Topex/Poseidon altimeter and the POP (Parallel Ocean Processor) model calculations of Semtner and Chervin (1992). The phase speeds vary qualitatively with latitude as predicted, yet effects of bottom topography, mean currents, and forcing by wind-stress curl apparently cause some quantitative disagreement. We are at an early stage of understanding the rich structure seen in this field, but the role of the β-effect and relevance of Rossby wave dynamics seems to be clear. The global fields provide space-time structure for ENSO cycles, annual cycles, decadal climate variability of the general circulation, and oceanic heat storage.

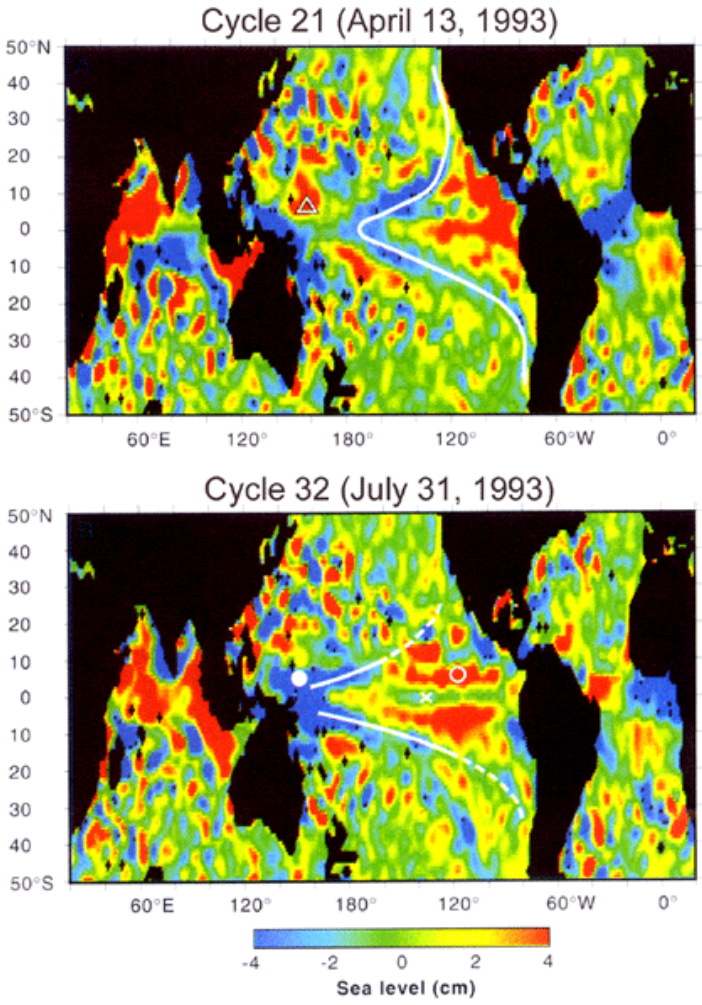

Figure 14.15 Snapshots of sea-surface height anomaly, spatially smoothed to emphasize scales longer than those of mesoscale eddies (Chelton and Schlax, 1996).

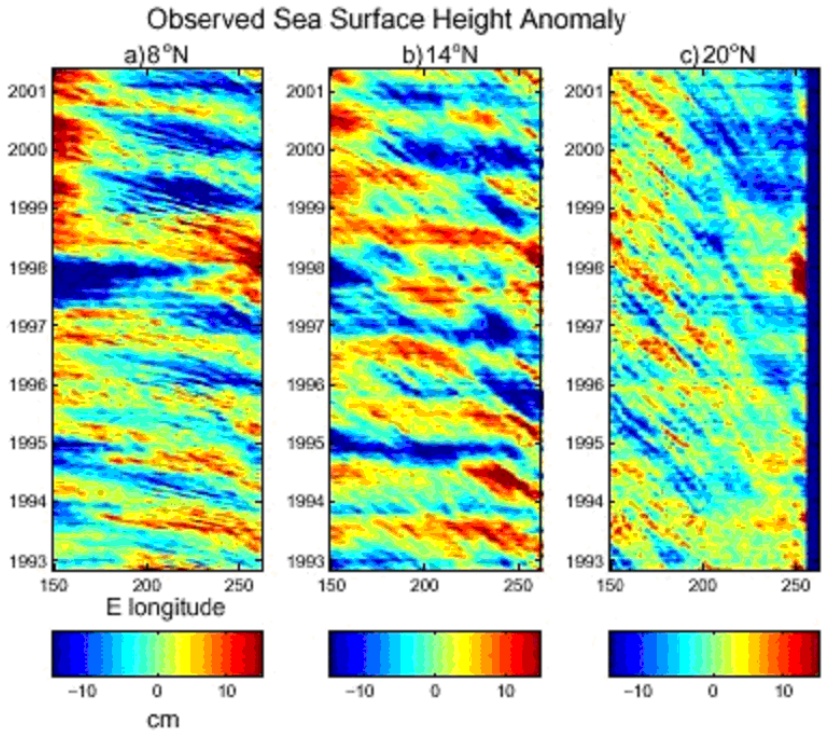

Figure 14.16 Satellite altimeter observation of the sea-surface height field in the North Pacific, Chelton and Schlax (1996), Kelly and Thompson (2003) as time-longitude plots. Note the well-defined westward propagation speeds, which increase with latitude. Time progresses upward, and we are watching over 8 years. These waves are slow! They are most likely n=1 mode Rossby waves in the upper ocean, with the thermocline acting as a 'free surface' with a reduced gravity, so that $\lambda_{BC} \cong 50$ km or so. There is a strong signal at annual period as well as shorter period activity.

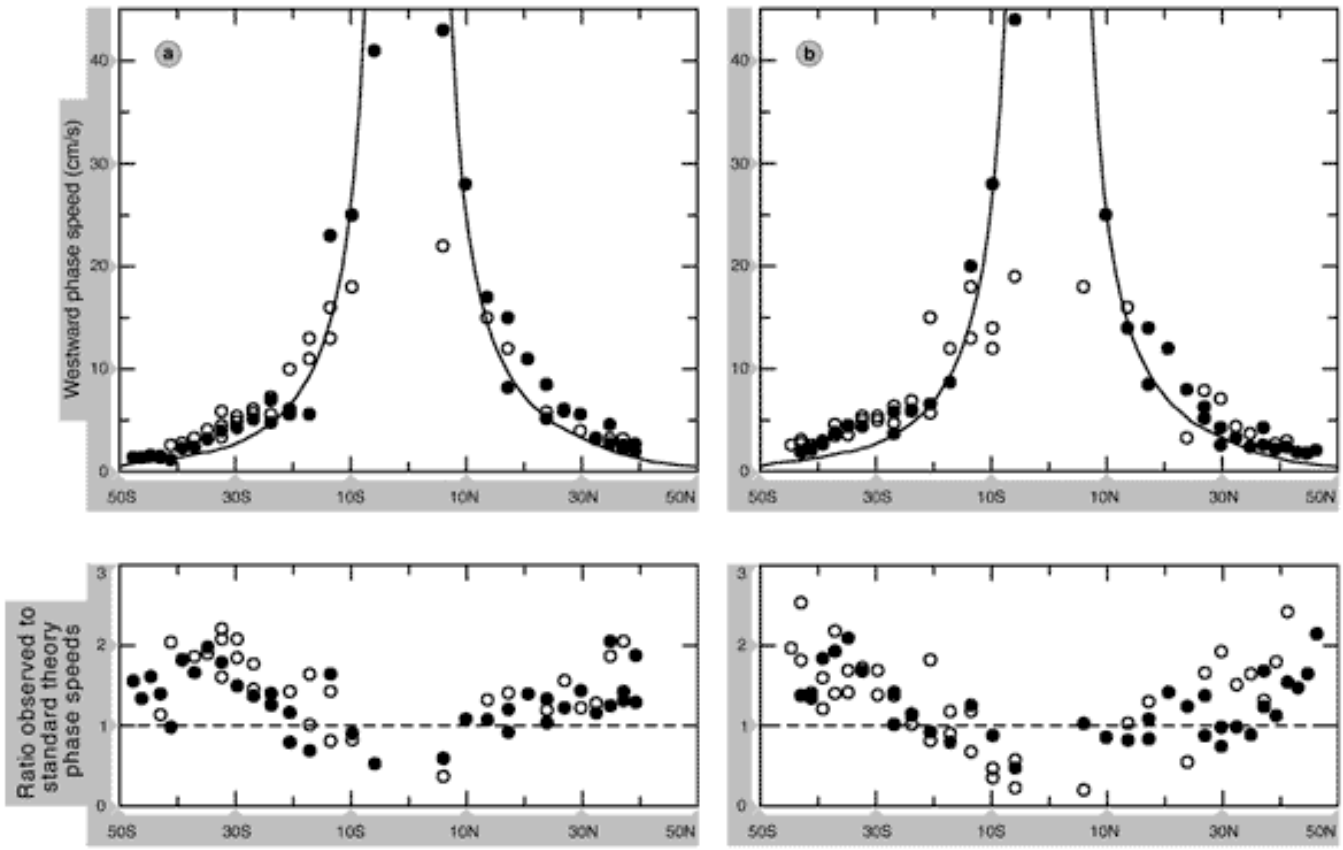

Figure 14.17 Phase speeds estimated from 7 years of T/P data (a) and 3 years of Run 11 of the POP model (b) based on the classical theory (solid line) and from the T/P and POP SSH fields in the Pacific (solid circles) and the Atlantic and Indian oceans (open circles). The ratios of the observed phase speed to the phase speed predicted based on the classical theory is shown in bottom panel (Chelton and Schlax, 1996).

A simplified view of long baroclinic waves. The long-wave limit $L >> \lambda_{BT}$ of the baroclinic wave problem applies to much of the eddy, wave, and circulation structure of the oceans, because λ_{BT} ranges from roughly 100 km to less than 10 km at high latitude. This limit leads to such a simple equation (and hopeful suggestions of simple solutions) that its physics must be essentially different from the general case of PV conservation. We have seen that the relative vorticity then makes a negligible contribution to PV, $O((\lambda_{BT}/L)^2, (\lambda_{BC}/L)^2)$ for the respective barotropic and baroclinic waves. This means that 'stiff-column' dynamics inherent in the Sverdrup balance, Chap. 12, becomes valid. For clarity let us think of a laboratory experiment (Fig. 14.18) in which the β-effect is provided by an analogous slope of the upper and lower rigid boundaries. The fluid is comprised of two layers of equal mean thickness, and density difference $\Delta\rho$. The rotation axis is vertical (aligned with the fluid columns). We use the words 'north' and 'west' to correspond to the positive y- and negative-x directions. With the pattern of velocities sketched on the figure,

the north-south velocity forces a vertical velocity, just as if the columns were metal rods. This moves the interface vertically, causing the pattern to propagate westward. Thus the vortex-stretching and advection of neighboring fluid, so active in barotropic Rossby waves, is absent here. It is a 'kinematic' sort of wave, without much classical vorticity dynamics. An inclined-plane relation connects vertical and horizontal velocity:

$$2\alpha v_2 = \eta_t \qquad (14.29)$$

where α is the magnitude of the slope of both top and bottom, and w_i is the vertical velocity of the interface. [This may be derived by expanding the 'shallow-water' expression for mass conservation in the form

$$\frac{D\eta}{Dt} = \nabla \bullet (h_1 \vec{u}_1) = -\nabla \bullet (h_2 \vec{u}_2)$$
$$h_1 = \tfrac{1}{2}H - \eta, \quad h_2 = \tfrac{1}{2}H + \eta$$

by neglecting nonlinear terms and keeping α small. The total mean depth in the two layers is h_1 and h_2, respectively, and η is the vertical displacement of the interface.]

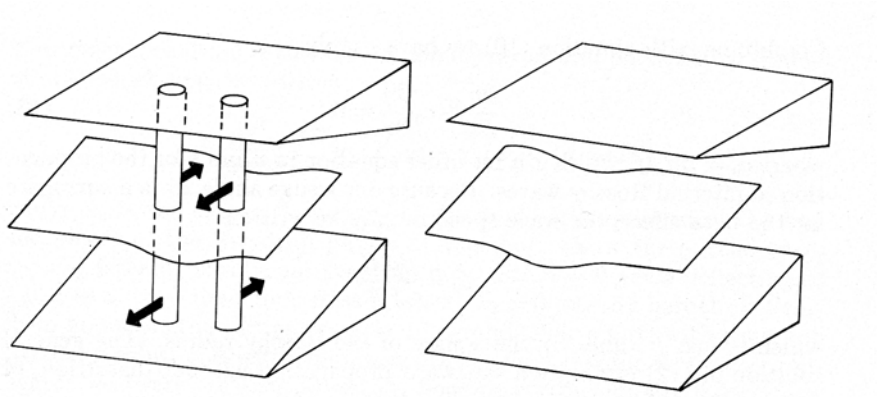

Fig. 14.18 View from the southeast of a long, baroclinic Rossby wave in a two-layer fluid. This represents a laboratory experiment with upper and lower boundaries sloping to provide a variation in mean potential vorticity in each layer. In the left panel, with the velocities chosen, columns of fluid move north and south, in a pattern allowed by thermal-wind shear at the interface. Being stiffened by planetary rotation, they force the density interface downward at the left and upward at the right. The result is a propagation of the pattern to the left ('westward') as seen in the right panel.

Because the top and bottom are rigid, and the fluid acts as if it were, the average north-south velocity must vanish:

$$v_2 = -v_1$$

and the thermal-wind balance (in the form of Margules two-layer relation) is

$$v_1 - v_2 = 2v_1 = -(g'/f)\eta_x \qquad (14.30)$$

where $g' = g\Delta\rho/\rho_0$. Eqns. (14.29) and (14.30) combine to give

$$\eta_t + c_0\eta_x = 0\,.$$

where $c_0 = \alpha g'/f$. Because the same PV gradient is provided by β and a bottom slope obeying $\beta = f\, h_y/h$, we can express the wave-speed in terms of this effective β:

$$c_0 = \beta g' H / 4 f^2 = \beta \lambda^2 \qquad (14.31)$$

where λ is the Rossby deformation radius. The general solution of (14.31) is a simple westward propagation of initial conditions $\eta = \eta_0(x,y)$ without the distorting effects of dispersion,

$$\eta = \eta_0(x + c_0 t, y) \qquad (14.32)$$

The connection with the spherical Earth comes from the 'stiffness' rules described earlier, and from application of the ideas of Chap. 12 to a two-layer fluid on a sphere. This 2-layer model of the β-plane can be built as a physical laboratory experiment, and Ohlsen and Hart (1989) have carried out meticulous observations of baroclinic waves with the β-effect. Unfortunately it is not easy to extend the laboratory analogy to a continuously stratified fluid, because the Ertel potential vorticity of such a fluid is uniform along isopycnal surfaces (which lie parallel to the paraboloidal equipotential surfaces of a rotating laboratory experiment), although exotic ferromagnetic fluids may one day make this possible (Ohlsen and Rhines, 1997).

A simplified expression for the set-up of the wind-driven ocean circulation.
Incorporating wind-forcing in this two-layer model, leading to a vertical velocity $w_e(x,y,t)$ at the top of the fluid, we have the forced wave equation

$$\eta_t + \frac{\beta g' H}{4 f_0^2} \eta_x = \tfrac{1}{2} w_e$$

If the fluid is initially at rest and the windstress suddenly switches on at time t=0, the general solution is

$$\eta = c_0^{-1} \int_x^{x_E} (w_e(x', y) - w_e(x + c_0 t, y))\, dx'$$

This, when plotted, is an intriguing pattern in which the initially flat interface and motionless fluid gradually separates into two dynamical parts: a westward propagating circulation with the shape of the Ekman forcing and, left behind, a steady circulation of the opposite sign which is the steady Svedrup flow. The transient flow propagates out of the picture to the west as no lateral, coastal boundaries are present here. As it departs the region of wind forcing it shuts down the horizontal circulation below the interface and doubles the circulation above the interface. In the solution above, there is an implicit appeal to the fast propagation of barotropic Rossby waves. Even though absent from the equations, we assert that once the wind begins, a barotropic mode Rossby wave is generated and propagates rapidly, 'instantaneously' in these dynamics, out of the picture. Left behind are the initial conditions for the baroclinic wave and circulation, with $\eta = 0$ yet a barotropic velocity field satisfying the Sverdrup relation,

$$v_1 = v_2 = (f_0 / \beta H)^{-1} w_e(x, y)$$

The propagation of baroclinic Rossby waves is extremely slow (Fig 14.14), yet they may still exert control on the set-up and variability of general circulation, and their propagation speed increases rapidly as one approaches the Equator (as $\beta\lambda^2$ varies like (latitude)$^{-2}$ near the Equator; close to the Equator it is replaced by the 'Equatorial Rossby Radius', $\sqrt{(c_0/\beta)}$). Baroclinic Rossby waves are essential components of el Niño-Southern Oscillation cycles in the tropical Pacific, one of the dominant interannual climate cycles on Earth.

14.11 *Baroclinic Rossby waves in a stratified atmosphere.* The atmospheric general circulation is global, with seemingly great dynamical connections between tropics and and higher latitude. In both the zonal and meridional circulation, Rossby waves and other related wave forms are active in establishing these connections, and indeed in shaping many aspects of the circulations.

Modern observations make it possible to make thorough, global, 4-dimensional analyses of the atmospheric circulation, including the eddy-, wave- and jet- structures down to a 100 km or so horizontally and roughly 500m vertically. The wintertime mean dynamic height field at 300mb in the upper troposphere is plotted in Fig. 14.19, and superimposed on it, the absolute vorticity, $\zeta + f$. While this rather subtle long-wave pattern (roughly two ridges and two troughs round a latitude circle) does not much resemble the simple standing Rossby wave in Fig. 14.14, they have much in common. Low pressure troughs sit in the lee of the Himalayan Plateau and Rocky Mountains. Continuation of the pressure field down to the surface verifies that this weakly baroclinic mode exerts a strong wave-drag on the topographic slopes.

Figure 14.19. Streamlines (solid) and absolute vorticity, ζ + f, averaged at 300 HPa level in the upper troposphere (figure from Lau, 1979). The deviation of the streamlines from circles is a wave pattern analogous to Figure 1. If this were simply barotropic Rossby waves, the dashed and full lines would coincide. Continents are shown with dotted curves; North America is at the bottom of the figure.

The analysis developed so far will, with slight modification, act as a model for atmospheric Rossby waves. What distinguishes them is the large density gradient in the atmosphere, and its compressibility, compared with the much more 'Boussinesq' ocean, where the density changes by perhaps 2% from surface to sea floor. The greater stratification of the atmosphere, such that $\lambda_{\mathbf{BC}}$ ~1000 km there rather than 10 to 50 km as in the oceans, combined with the open geometry of the atmosphere, yield energetically dominant flows with horizontal scales of 1000km-5000km. Also distinguishing them is the large zonal flow of the atmosphere, with forcing provided both by continental topography, and by land-sea contrast in heat flux and fresh-water flux. We nevertheless derive the wave equation afresh.

Rossby waves on a mean, stratified zonal circulation. A compressible fluid has a mass conservation equation

$$\frac{D\rho}{Dt} = -\rho \nabla \bullet \vec{u}$$

with equation of state written in terms of the adiabatic sound speed c_s as

$$\frac{D\rho}{Dt} = c_s^{-2}\frac{Dp}{Dt} = c_s^{-2}(\frac{\partial p}{\partial t} + \vec{u}_h \bullet \nabla p + w\frac{\partial p}{\partial z})$$

u_h is the horizontal velocity. Thus, because the vertical hydrostatic pressure gradient is so large,

$$\nabla \bullet \vec{u} \cong (\frac{g}{c_s^{\,2}})w$$

This leads to vertical vorticity- and potential vorticity equations that are very similar to their Boussinesq counterparts. We will derive potential vorticity equation

$$\frac{D_g q}{Dt} = 0 \quad q = f_o + \beta y + f_o^{-1}(\nabla_h^{\,2}\Phi' + \frac{1}{\rho_*}(\frac{f_o^{\,2}}{N_*^{\,2}}\rho_*\Phi_{z^*})_{z^*}) \qquad (14.33)$$

where $\Phi'(x,y,z_*)$ is the perturbation to the geopotential height gz. q is very close to the exact Ertel-Rossby potential vorticity, but with a slight correction, as described in Chap. 13. Here we are using log-pressure vertical coordinates, (x,y,z) -> (x,y,z_*)

$$z_* = -H_s \log(p/p_r) \quad \rho_* = \rho_r e^{-z_*/H_s} = \frac{\rho_r}{p_r}p = \rho\frac{\partial z}{\partial z_*} \quad N_*/N = p/\rho_o g H_s = T_o/T_r = \frac{\partial z}{\partial z_*}$$

The second relation corrects a minor error in Gill (6.17.29). Here the subscript $(\,)_o$ refers to the rest state, as in the larger vertical stratification $\rho_o(z)$; and $(\,)_r$ refers to constant reference values like ρ_r being the rest state density at 1000 mb. The scale height H_s is defined as p_r/ρ_r. z_* is very close to the usual z-coordinate. If we keep in mind an isothermal/perfect-gas atmosphere as a comparison state, then the log-pressure coordinate z_* is simply proportional to true height z, and N_* is just N (because the rest-state pressure and density then vary like exp(-gz/RT)).

The velocity (u,v,w) becomes $(u,v,dz_*/dt)$, where the last term is w_*, is the time rate of change of the log-pressure following a fluid parcel. In place of pressure we use geopotential height $\Phi(x,y,z_*) \approx gz$. It gives an oceanographer an uneasy feeling to see a motion-dependent variable like pressure used as an independent variable, but the overwhelming hydrostatic pressure balance helps to make this acceptable. The appearance of ρ_* and N_* in the equation would seem to suggest extra nonlinearity, since both would change when the fluid is in motion. This would be true, but the small variations in these variables are scaled out of the equation, for the hydrostatically balanced mean pressure and density are the dominant parts.

Digression concerning pressure coordinates. Our normal vertical velocity, w, is dZ/dt where Z(t) is the height of a marked fluid parcel [Z is a Lagrangian quantity]. You can get the right answer in (x,y,z) coordinates in terms of the independent variable z (= vertical height), as "Dz/Dt = $\partial z/\partial t + u\partial z/\partial x + w\partial z/\partial z$ = 0+0+w", though it's a bit poor use of notation, because the independent variable z is not a function of x,y,z that can be differentiated) . In the new system the pseudo-vertical velocity is $\varpi = dP/dt$ for (x,y,p) pressure coordinates or dZ_*/dt for log pressure coordinates where P(t) is the Lagrangian pressure of a

marked fluid parcel and $Z_*=H_s\log(P/p_r)$ is the corresponding log-pressure (or, as before you can get the right answer with independent variables x,y,p, "$Dp/Dt \equiv \partial p/\partial t+u\partial p/\partial x+\varpi\partial p/\partial p = 0+0+\varpi$" and x,y,$z_*$, "$Dz_*/Dt$" though it's a bit inconsistent).

. The log-pressure vertical coordinate, and its relative, the simple pressure coordinate, are motivated in part by the simpler mass conservation equation: the mass conservation

$$\partial u/\partial x+\partial v/\partial y+\partial w/\partial z=-(1/\rho)D\rho/Dt$$

becomes non-divergent in pressure coordinates

$$u_x + v_y + \varpi_p = 0.$$

In log-pressure coordinates, mass conservation is

$$u_x + v_y + w^*_{z^*} = w^*/H_s$$

With the fluid so close to hydrostatic force balance in the vertical, the connection between z, z_* and p is quite close. Notice however that when we need physical vertical velocity, (to apply the lower boundary condition) then it has to be transformed carefully. We have

$$\varpi = \frac{Dp}{Dt} = p_t + up_x + vp_y + p_z$$

expressed in 'old' x,y,z system.The horizontal advection of p vanishes to order Rossby number in a quasi-geostrophic flow, so with hydrostatic balance

$$\varpi = -g\rho w + p_t$$
$$= -g\rho w + \rho f_0 \psi_t$$

where the righthand side derivatives are in the x,y,z system (or see Holton (2003)). Manipulation of these give the various mass conservation equations above, or one can derive it in x,y,p coordinates from scratch. Write

$$\varpi_p = (\frac{D\rho}{DT})_p = -\frac{1}{\rho g}(\frac{Dp}{Dt})_z = -\frac{1}{\rho g}(\frac{Dp_z}{Dt} - w_z p_z) = w_z - \rho^{-1}\frac{D\rho}{Dt}$$

for quasi-geostrophic flow. Thus at a rigid horizontal surface, the ground, w vanishes but ϖ does not. The vertical velocity-like variables in the three coordinate systems are related by

$$w_* = (gH_s/RT)w - (f_oH_s/RT)\partial\psi/\partial t$$
$$= -H_s\varpi/p.$$

14.12 *Vorticity dynamics.* The corresponding vertical vorticity equation is

$$f_o^{\,2}(w^*_{z^*} - \frac{w_*}{H_s}) = \beta\Phi'_x + \frac{D_g}{Dt}(\nabla_h^{\,2}\Phi') \qquad (14.34)$$

which has just one new term due to compressibility. The density equation is

$$N_*^{\,2}w_* + \frac{D_g}{Dt}(\Phi'_{z^*}) = 0$$

The general quasi-geostrophic potential vorticity equation in log-pressure coordinates comes from eliminating w_* from the above two equations. This is most simply done by rewriting the LHS of (14.34) as

$$f_o^2 e^{z^*/H_s}(w_* e^{-z^*/H_s})_{z^*}$$

and substituting the definition $\rho_*=\rho_r \exp(-z_*/H_s)$. The result is

$$\frac{D_g q}{Dt}=0; \quad q=f_o+\beta y+\frac{1}{f_o}(\Phi'_{xx}+\Phi'_{yy}+\frac{1}{\rho_*}(\rho_*\frac{f_o^2}{N_*^2}\Phi'_{z^*})_{z^*})$$

Now we want to look at waves on mean zonal flow, defining zonal means and perturbations:

$$q'_t+Uq_x+v\bar{q}_y=0 \qquad q=\bar{q}(y,z)+q'(x,y,z_*,t) \tag{14.35}$$
$$\bar{q}_y=\beta-U_{yy}-\frac{1}{\rho_*}(\frac{f_o^2}{N_*^2}\rho_* U_{z^*})_{z^*}$$

The major new feature is the huge variation in $\rho_*(z_*)$. There is a standard technique in o.d.e's, that removes a variable coefficient from the highest-differentiated term in the equation, by a change of *dependent* variable (in general in such an equation a term like $(a(z)\xi')'$ turns into φ'' by defining $\xi=\varphi\, a^{-1/2}$ so that in terms of the new dependent variable φ the operator $(a\xi')'=a^{1/2}(\varphi''+(1/2\, a'^2/a^2-a''/a)\varphi)$. In this spirit, let

$$\Phi'=\Psi(z)e^{z_*/2H_s}\, e^{(ikx+ily-i\omega t)} \Rightarrow \Psi_{z^*z^*}+m^2\Psi=0$$
$$\text{where } m^2=(\frac{N_*}{f_o})^2(\frac{\bar{q}_y}{U-c}-k^2-l^2) \text{ and } c=\omega/k \tag{14.36}$$

Eqn. (14.35) is more general than Eqn. (14.36), where we suppose U to be gradually varying in y relative to the meridional scale of the waves in order that the equation be separable. The vertical velocity is related to the geopotential through the density equation

$$N_*^2 w_*+(\frac{\partial}{\partial t}+U\frac{\partial}{\partial x})\frac{\partial\Phi'}{\partial z_*}-\frac{\partial U}{\partial z_*}\frac{\partial\Phi'}{\partial x}=0$$

with the last term coming from the horizontal advection of the mean temperature, as expressed by the thermal wind. This is important when it comes time to apply boundary conditions.

Now for ultimate simplicity take U and N_* to be constant, so that

$$m^2=(N_*^2/f_o^2)(\frac{\beta}{U-c}-k^2-l^2)-\frac{1}{4H_s^2}$$

or

$$\omega-Uk=\frac{-\beta k}{k^2+l^2+\frac{f_o^2}{N_*^2}(m^2+\frac{1}{4H_s^2})}$$

This is identical to the oceanic Rossby wave equation but for the compressibility term. Notice the *barotropic* mode for m=0, in which the ridges and troughs of pressure are vertical, yet there is exponential decay of energy upward (despite the exponential increase in pressure perturbation with altitude). In this case the dispersion relation is exactly that of a single layer of constant density incompressible fluid *with a free surface*. The nature of the barotropic mode waves is very dispersive [phase speed depends on the wavevector (k,l) and group velocity does not point in the direction of the wavevector (k,l)]. But it changes radically when the lateral scale of the waves exceeds $N_* H_s / f_o$, or typically 1500km. Then the barotropic mode begins to be non-dispersive, with $c-U = -4\beta N_*^2/f_o^2$. The waves propagate purely westward relative to the mean flow, at a single speed. This kind of behavior encourages strong resonance for the stationary waves at latitudes where U is given by the righthand expression.

Thus, in the general case, baroclinic Rossby waves propagate relative to the westerly wind, at speed βL^2 determined by L, the *smallest* of 3 length scales: the Rossby deformation radius N_*/fm based on the vertical scale of the wave 1/m; the horizontal wavelength-scale $(k^2+l^2)^{-1/2}$, and the scale $N_* H_s/f_o$, essentially the Rossby radius based on the density scale height. It is usual to plot the frequency as a function of (k,l,m) wavenumbers. This can be done a number of ways, for example fixing a few values of m and plotting ω(k,l;m). This has the shape of a 'witch's hat', similar to Fig. 14.13, a lopsided peaked hill with a broad 'brim'. The altitude contours (ω=const.) are circles lying to in the left half plane k<0. The maximum frequency lies on the l=0 axis, where k^2 is equal to the two stratification dependent terms. The *gradient vector* of the witch's hat is the horizontal group velocity.

Another way to do this is to plot surfaces in fixed ω in the (k,l,m) plane. For the special choice ω=0 (or c=0, that is stationary waves) these are tall ellipsoids symmetric about the vertical, m-axis, with radius in the m=0 plane, call it k_c, given by $(\beta/U - f_o^2/4N_*^2H_s^2)^{1/2}$. Waves with horizontal wavenumber $\sqrt{(k^2 + l^2)} > k_c$ cannot propagate, and if excited they will be evanescent (exponentially decaying) in the vertical. The possible solutions are

$$U = \frac{-\beta}{k^2 + l^2 + \frac{f_o^2}{N_*^2}(m^2 + \frac{1}{4H_s^2})}; \quad or \quad k = 0$$

$$m^2 = (\frac{N_*}{f_o})^2(\frac{\beta}{U} - k^2 - l^2) - \frac{1}{4H_s^2}; \; or \quad k = 0$$

This is quite a remarkable result. We can rescale the figure by using 'Prandtl ratio stretching of the horizontal relative to the vertical'; plotted with axes $(k,l,f_o m/N_*)$ the figure becomes a simple sphere! Thus the possible waves which are stationary in a uniform zonal flow U have wave-vectors of the same length, lying in all possible

horizontal and vertical directions. The dual of this stretched k-space is a stretched x,y,z space. The group velocity, which tells us the energy propagation direction and speed for rays of Rossby wave energy, lies normal to the sphere, thinking of the rays propagating in $(x,y,N_* z /f_o)$ space. If we draw a zonal section in stretched space $(x, z_* N_*/f_o)$ the orientation of the phase lines (wave crests) will be perpendicular to the rays of energy propagation (the group velocity). Upward energy propagation requires a wave-vector pointing westward/downward, implying wave-crests that tilt westward/upward. The other possible root, k=0, describes nearly horizontal velocity perturbations that can propagate upstream or downstream from a region of forcing. They are nearly-zero-frequency Rossby waves that play the role of wakes and upstream blocking flows, and have large group velocity despite their small frequency.

The upstream tilt of the wave-crests of stationary Rossby waves is one of the most famous results of dynamical meteorology. It is indeed observed (Fig. 14.20), and it carries with it strong implications to poleward heat flux, upward flux of zonal momentum and meridional PV flux by the waves. This momentum flux opposes the strong polar cyclonic vortex in the stratosphere and, in most northern hemisphere winters, causes the 'sudden stratospheric warming' which is really the sudden braking of the vortex, and adiabatic relaxation of the potential temperature. While the quasi-barotropic, $m = 0$, mode has no such tilt, excitation by the topography apparently picks out a range of values of m.

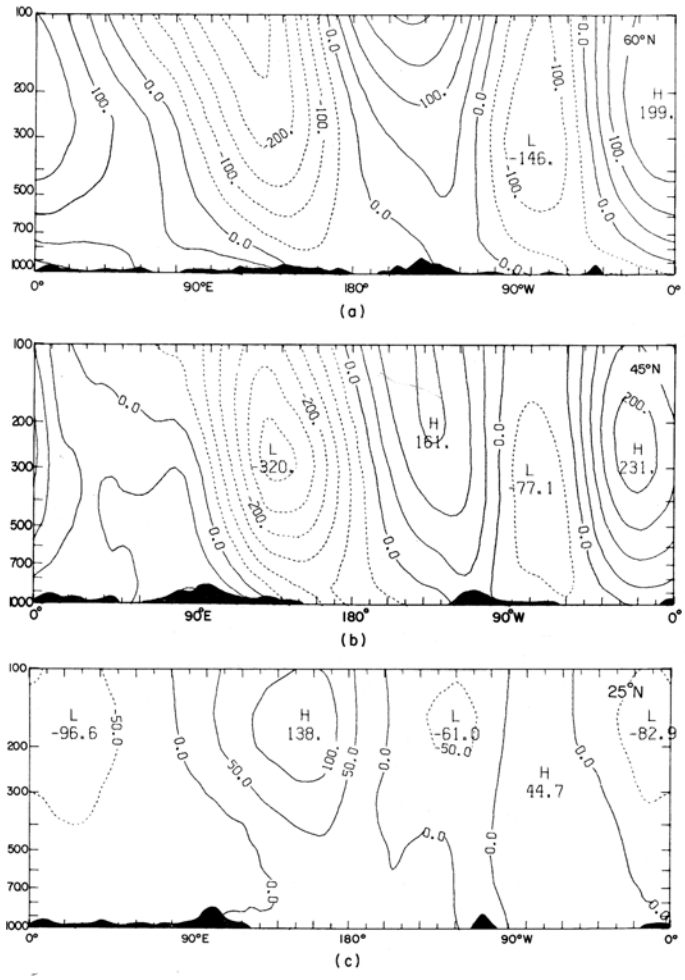

Figure 14.20. Cross-sections of the geopotential height (in meters) of the atmosphere at 60^0N (a, upper); 45^0N (b, middle) and 25^0N (c, lower). This is the flow averaged in time during the winter season. Here the vertical axis is pressure-level and the horizontal axis is longitude. To a good approximation this can be viewed as a plot of pressure with respect to actual altitude and longitude (figure from Lau, 1979). The flow in Figure 14.19 cuts through this figure at the 300 Hpa level. A smoothed profile of mountain topography is shown, which shows low pressure on the lee slopes of the topgraphic rises.

What would the wave pattern look like, due to a source of energy in a smallish region at the ground? The symmetry of the spherical pattern tells us that the wave crests would also be spheres in the stretched space. But the group velocity directions are such that the spherical wave crests would appear only in the lee of the mountain, with an eastward (westerly) wind. In unstretched physical space the waves would be ellipsoids, long and skinny in the x-direction, pointing like half-sausages in the lee of the mountain. This is an outline of the 'ray theory' of stationary Rossby waves, involving techniques that can be found in Lighthill's text on waves (1978). Hoskins and Karoly (1981, 1982) and many other authors pursue other aspects of the ray theory, following the waves through major changes in zonal velocity and latitude. Generation by flow over topography may

select out some favored band of horizontal wavenumbers. If the favored k is significantly less than k_c we will see very tilted wavecrests in the either streteched or real coordinates. If is close to k_c we will see quasi-barotropic waves with nearly vertical wavecrests (or constant-phase surfaces).

14.13 *Vertical penetration.* Charney and Drazin (1961) noted this expression for m^2, the 'refractive index' of the atmosphere. Taking c=0, we see that upward propagating waves, with $m^2 > 0$, occur only for westerly (eastward) winds that are 'slow enough', at a given east-west wavenumber, k, or for waves that are 'long enough', for a given, fixed westerly windspeed. The sizable westerlies dimininish upward into the stratosphere in summer, where easterlies are instead found. Planetary waves that are stationary cannot escape the troposphere then, for they are reflected where m^2 changes sign. In winter, however, the radiative cooling of the stratosphere drives a zonal circulation in the form of a polar vortex with strong westerlies exceeding 60 m/sec in the zonal average, at 60km altitude. This 'polar night jet' invites upward propagation, and the wintertime troposphere has intense westerlies itself, making much large scale energy available. Observations indeed show ample long-wave energy reaching into the stratosphere then. Typically waves of lateral scale > about 1500 km escape upward. The ray theory (short-wavelength approximation, which doesn't sound very adequate for this kind of motion) shows interesting and complex paths that lean equatorward (Karoly and Hoskins, 1982).

To see more deeply into this problem, we want to reconsider the wave equation, fixing the east-west wavenumber, k, and looking at the remaining general structure in the meridional, y-z plane. Consider for simplicity the case of uniform N_*^2. For stationary waves, c = 0, Eqn. (14.35) with mean westerly wind U(y,z), let $\psi = \exp(ikx)\exp(Z/2H)\,\Phi(y,z)$, giving

$$\Phi_{yy} + \Phi_{Z^*Z^*} + \nu^2\Phi = 0$$

$$\nu^2 = \left[-\lambda^2 - k^2 + U^{-1}\frac{dq}{dy} \right];\ \lambda = f/2NH$$

In the meridional plane, the rather complex propagation problem for a single zonal wave reduces to a familiar Helmholtz equation; although Rossby waves are dispersive, they propagate in this reduced problem like non-dispersive light or sound (keeping in mind hat their wavelength in this plane should be small for literal ray-tracing solutions to be effective). Here ν^2 is the index of refraction for the waves; simple refraction occurs, in which rays bend toward regions of large index of refraction (that is, regions of slow wave-speed), and their paths can be sketched on a plot of ν^2. Solutions of this equation are wave-like where ν^2 is greater than zero, and waves cannot penetrate regions where ν^2 is negative;

only a small tail of the disturbances reaches inside such regions. In particular, the waves can penetrate only where U falls in the range

$$0 < U < \frac{dq/dy}{k^2 + \lambda^2}.$$

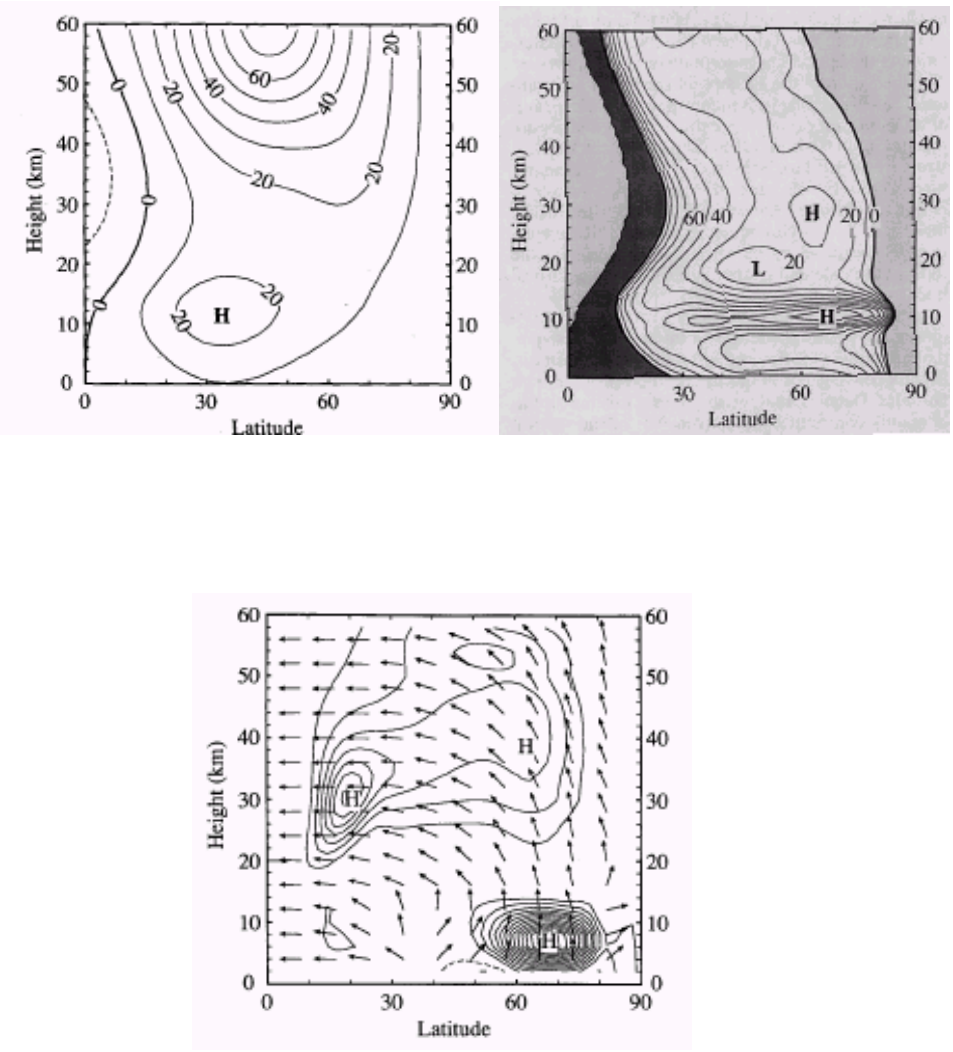

Figure 14.21 Numerical model experiments from Chen and Robinson (1993). First panel: mean east-west wind used in the model. Second panel: refractive index for steady zonal wavenumber 2. Dark band has high positive values. Third panel: propagation paths (group velocity vectors) for idealized Rossby waves, refracting toward the Equator (toward large refractive index, or large wavespeed) with height. Contours show the convergence of the Elliasen-Palm flux, which exerts a westward force on the general circulation; it is particularly strong in the tropics where U goes to zero.

14.14 *Refraction and wave-guides for the quasi-barotropic mode.* Rossby waves in the m=0 mode follow horizontal propagation pathways ('rays') in an approximate sense,

and these rays are bent by variations in large-scale PV from the time-averaged winds, the thermal structure, and topography of the solid Earth. Preferred paths ('waveguides' or 'ducts') of the waves are created in this way, for example in the core of the westerly winds, along the Equator, and in the upper polar troposphere.

Some of the topographically induced standing wave patterns of the atmosphere are at least in part are attributable to Rossby wave dynamics. Consider now the kind of perturbation to the mean standing-wave circulation arising from an additional source of waves, as in Figure 14.22. For example, during el Nino events in the Pacific, the extraordinarily warm sea-surface temperature can excite waves in the atmosphere passing above, and the 'Pacific-North America' or PNA pattern resembling the model, Fig. 14.22, is the dominant empirical orthogonal function of the Pacific-North America sector. Yet it is found that the wave pattern generated is sensitive to the location (east and

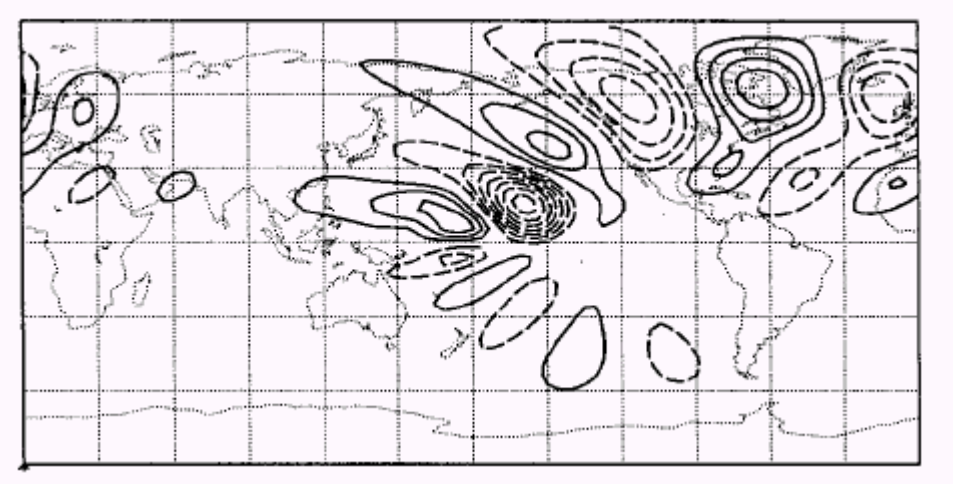

Figure 14.22. Trains of Rossby waves propagate in both hemispheres from a modeled source of cumulus-convective heating in the western equatorial Pacific. The model takes the observed, fully three-dimensional structure of the circulation, and calculates the change in the winds arising from tropical heating by the warm ocean (figure from Jin and Hoskins, 1995). The waves move eastward along (very approximately) great-circle paths. Plotted contours show the north-south wind (not including that of the time-averaged winds) in the upper troposphere, contour interval 0.5 meters per second.

west) of the forcing region; this would not be the case for a simple Rossby wave problem. We must generalize the restoring effect for Rossby waves to include pv gradients in the mean winds themselves. In equation (6) β is replaced by $q_y = \beta - U_{yy}$ for this barotropic model. Now consider what this does. The *curvature* of the U(y) profile (which is the gradient of relative vorticity) is subtracted from β. For an easterly jet, the q(y) profile now has a 'flat spot' with small pv gradient cut like a plateau in the 'β hillside'. A westerly jet gains a concentrated gradient at the core of the jet. The concentration of vorticity in the mean flow augments the β-effect for the case of the westerly jet: it is the simple sum of the

planet-scale PV and the vorticity of the time-averaged winds that counts. The ray paths describing propagation of groups of short Rossby waves will bend toward from regions of large β^*, defined by

$$\beta^* = \left[\frac{dq/dy}{U} \right]^{1/2}$$

In this way waves will be deflected away from an easterly jet and trapped inside a westerly jet, which thus acts as a wave-guide.

Three panels in Figure 14.23 show the observed mean winter westerly wind, the barotropic pv gradient, dq/dy, and the effective restoring term β^*. Using similar, but three-dimensional fields from observations, linear Rossby waves were generated by a stationary

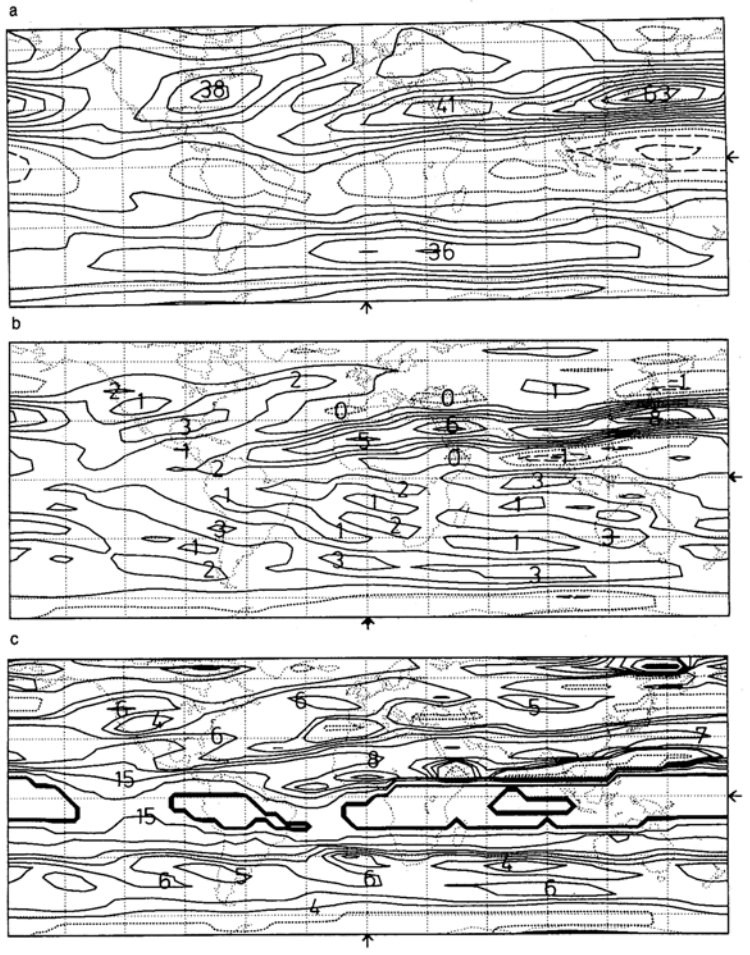

Figure 14.23 Upper: Mean westerly wind speed in northern-hemisphere winter. Middle: mean north-south barotropic potential vorticity gradient, β-$\partial^2 U/\partial y^2$. Note the large values in the mean westerly jets. Lower: effective restoring force for Rossby waves, β^*. Heavy line in lower panel is a concentration of high values of β^* at critical lines. Zero lines are dotted, negative are dashed. The Greenwich meridian is marked with an arrow. (From Hoskins and Ambrizzi, 1993).

source of vorticity {a twisting force in a small part of the fluid } as an exploratory computer experiment (Figure 14.24). The size of the forced region is about 30^0 of latitude. The waves indeed follow the westerly Northern Hemisphere jet. Preferred propagation into and out of the tropics occurs (Figure 14.23) at longitudes where the zonal winds are weak or westerly, rather than the more usual easterly winds. Lines along which U=0 lead to infinite values of β^*, and these 'critical lines' tend to reflect Rossby waves, after a certain amount absorption of their wave activity and momentum. Computer models are sensitive to the way such regions are handled, and to the levels of frictional damping assumed in their formulation, leading to lingering uncertainty about many features of the circulation.

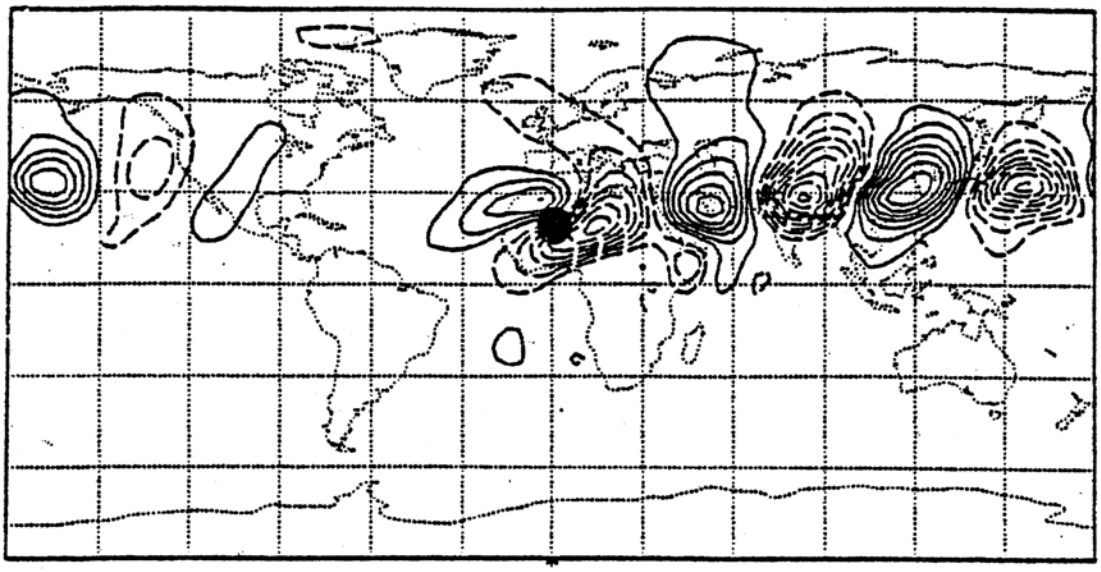

Figure 14.24. (From Ambrizzi and Hoskins, 1997). Meridional wind anomaly at day 10 for circular heat source at 20^0N, 0^0E, with December-January mean flow. This is a three-dimensional model calculation, but with a wave environment dominated by the barotropic pv, as in Fig. 14.23.

While the idea of Rossby waves having preferred wave-guides is attractive, and has been greatly developed in recent work (Branstator, 2002), a slightly different interpretation of this experiment is that the jetstream itself is prone to meandering. It has a strongly concentrated pv gradient, and when disturbed it develops stable but intense oscillations, which have both stable and unstable components. This is not quite the same thing as a Rossby wave-guide, and perhaps better describes the 'capture' of Rossby-wave energy by the underlying circulation.

This idea has been extensively developed, and it is found that the time-averaged winter winds can actively contribute to the wave field, exhibiting barotropic instability which can resemble a simple train of Rossby waves. Thus, in the PNA pattern, describing the atmospheric response to a warm tropical Pacific ocean, energy can be added to the wavetrain, transferred from the large-scale circulation, *en route* to North America. The weakly unstable modes are not easy to sort out because of the more rapidly growing baroclinic instabilities of the system.

A view of the development in time of a Rossby wave-train comes from a study of blocking patterns in the South Pacific (Renwick and Revell, 1999). Observations of winds at the 300 HPa level in the Pacific (Figure 14.25) show a structure that illustrates the development in time of Rossby wave propagation. Cumulus convection in the western tropical Pacific provides a large-scale pattern of divergent winds aloft. A train of cylones and anticyclones appears

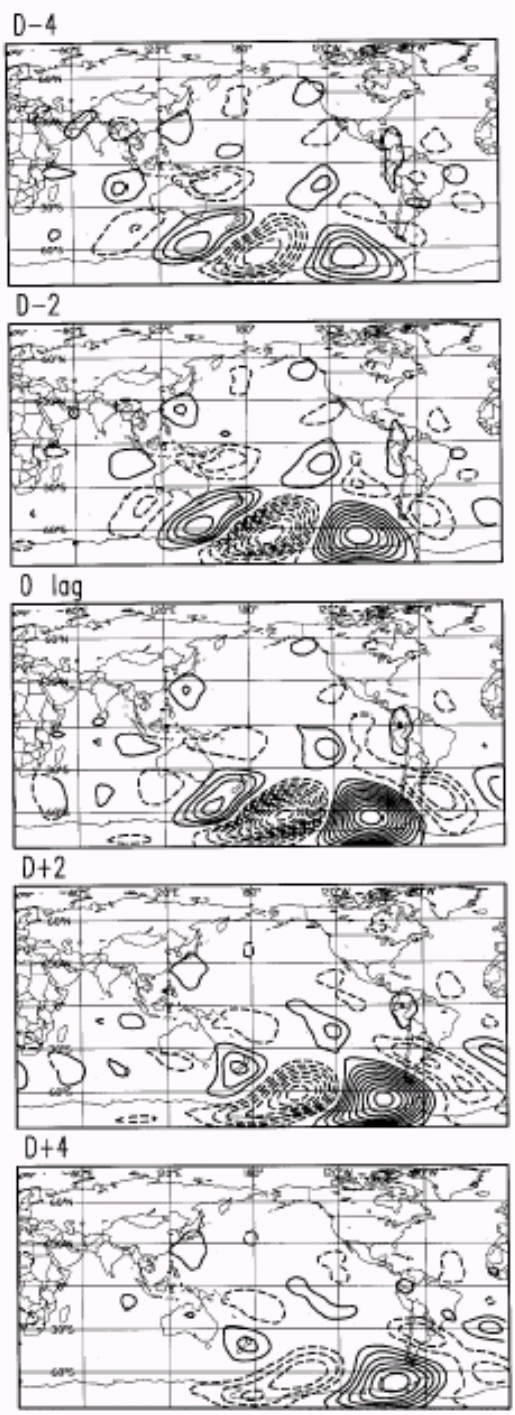

Figure 14.25 From Renwick and Revell (1999). A map showing the correlation between the north-south winds at 300 HPa level with the time series of southeast Pacific blocking. The panel labeled D – 4 represents the correlation pattern 4 days before maximum blocking, and the sequence proceeds in time to 4 days after peak blocking. The apparent wave train propagates from Australia southeastward across the Pacific. 'Blocking' here means a period of at least 5 days when the 500 HPa pressure is at least 0.5 standard deviation above the norm. The source of the wave train is thought to be cumulus convection in the western equatorial zone, and hence there is a strong correlation of warm el Nino periods with blocking patterns at higher latitude (SOI index:blocking index correlation reaches –0.8 during the past 15 years).

south of Australia and veers southeastward toward Chile, where it creates a lasting circulation cell strong enough to be called a 'blocking' pattern. The figure shows correlations of the winds with a time series that expresses this blocking: the winds themselves form a similar pattern. The waves arrive quickly (the speed of individual cyclones and anticyclones being about 5^0 of longitude per day, which appears to be slower than the southeastward development of the pattern as a whole). They decay slowly, influencing a vast region of the South Pacific and reaching into the South Atlantic. In a simpler fluid than the atmosphere, convection in the tropics would stimulate a more local response: here, waves cause a 'teleconnection' round half of the circumference of the Earth.

14.15 *Conclusions.* Because Rossby waves exist throughout the depth of the atmosphere and oceans, they are not 'superficial oscillations', but rather an expression of forces acting on the entire circulation. An isolated cyclone, if it is large enough in size and weak enough in wind velocity, will 'burst apart' into Rossby waves, forming new, elongated cyclones and anticyclones that gradually fill the fluid with motion (Figure 14.12). In this experiment the fluid itself oscillates gently, moving only slightly compared with the movement of the flow patterns. In the figure we have no mean westerly wind, so that most of the fluid is motionless. Stronger, more realistic cyclones do not radiate waves so efficiently, but the forces derived from the large-scale PV gradient are still at work, for example nudging hurricanes out of the tropics toward the poles.

When the close-in views of theoretically solved Rossby waves are expanded to the whole sphere, the waves tend to propagate along great-circle paths. While theory predicts their structure in the simplest circumstances, computer models must be employed if realistic mean wind patterns and land topography are included. The modelled Rossby-wave field generated by a similar pattern of equatorial heating by the ocean, Figure 14.22, has two branches propagating southeastward and northeastward from the western Pacific. The train of waves crossing North America is similar to the 'PNA pattern' which is associated with ENSO events (yet more will be said about this pattern in Chap. 15).

What features of the atmosphere are explained in some way by Rossby waves? Begun a century ago as an exploration of weak oscillations of the atmosphere and oceans (for example, the tides raised by moon and sun) the theory of Rossby waves now provides insight into the very heart of atmospheric (and oceanic) circulation dynamics. These waves are related to the meandering north and south of the westerly winds and, less directly, to the synoptic eddies that shape our weather. Rossby waves contribute to understanding the global pattern of these westerly winds, the enhancement of cyclonic disturbances in the lee of major mountain chains, the location and shape of storm tracks in the western

Atlantic and western Pacific, some forms of blocking and stagnation of air masses, the propagation of energy in long waves upward to the stratosphere, the transport of east-west momentum with these waves and the attendant deceleration and 'sudden warming' of the wintertime vortex that sits above the North Pole.

Along the Equator, oceanic heat and water-vapor drive cumulus towers which heat the larger scale atmosphere. The winds converge below and diverge above such a heat source, and air pulled into the pattern creates a pattern of circulation extending both east and west from the heat source. Rossby waves propagating westward from the region of forcing control the shape of this pattern to the west, while Kelvin waves describe the movement east of the heating. At a yet larger scale, the atmosphere signals the onset of el Niño in the tropical Pacific by sending a train of waves across North America: in simplest idealization these are Rossby waves (meanwhile, in the sea below, Rossby waves move westward along the Equator to reinforce the recurrence of el Niño). In the lower troposphere in summer great anticyclones fill the North Atlantic and Pacific oceans, and these are established by monsoon forcing (intense summertime warming of the land surface) yet organized and shaped by westward propagation of low-frequency Rossby waves. More distant relatives of the Rossby wave account for the basic instability of the primary, east-west atmospheric circulation: *baroclinic* instabilities which are the model of cyclonic storm development, tapping the potential energy of the atmosphere, and *barotropic* instabilities which tap the kinetic energy of the mean atmospheric flow. In the stratosphere, very large scale Rossby waves describe the undulations of the vortex sitting over the wintertime pole. They are excited by upward propagation of Rossby wave energy from the intense winter circulation below. The restoring force that gives us Rossby waves also inhibits mixing of fluid north and south, and in this way makes possible the ozone hole.

In the oceans, Rossby waves transmit energy preferentially westward, where it piles up along coastal boundaries. This leads, in the coming chapter, to theories of the Gulf Stream and other western boundary currents. Steered by bottom topography, Rossby/topographic waves are transmitted along wave-guides formed by the shallow continental shelves and continental rises, as well as mid-ocean ridges. The response of the ocean to forcing by wind-stress and buoyancy forcing involves both fast barotropic and slow baroclinic waves. Over complex topography the equations are no longer separable, so that Rossby waves can jump from one vertical mode to another. A family of trapped 'edge-' and 'bottom-trapped' topographic waves exists over sloping topography. Despite this complexity, the long-wave limit, with *non-dispersive*, westward propagating baroclinic Rossby waves, applies to a vast range of phenomena of lateral scale greater than the Rossby deformation scale, λ_{BC}.

Before being completely carried away by the potency of the idea of linear Rossby waves, however, we have to warn that they are in competition with other forms of flow, particularly with turbulent, large-amplitude winds which are not waves at all. At the scale of the larger weather systems, the 'flow' dynamics and the 'wave' dynamics are nearly equal in importance. Yet it experience shows that the effects of linear Rossby waves persist at surprisingly large amplitude, even in the presence of nonlinear effects: steepening of the waves, refraction and change in vertical mode structure. This is the subject of our most 'advanced' material in this text, Chapter 17.

14.16 *Historical notes.* Large-scale waves on a rotating sphere were predicted with mathematical theory at the end of the 19th Century by Hough and Margules. Bernard Haurwitz (Figure 14.26), after leaving Germany in the early 1930s, derived the essential properties of these modes in a 1937 paper. His status as 'enemy alien' in the USA in 1942 did not prevent the Army Air Corps from asking him to direct a research program on

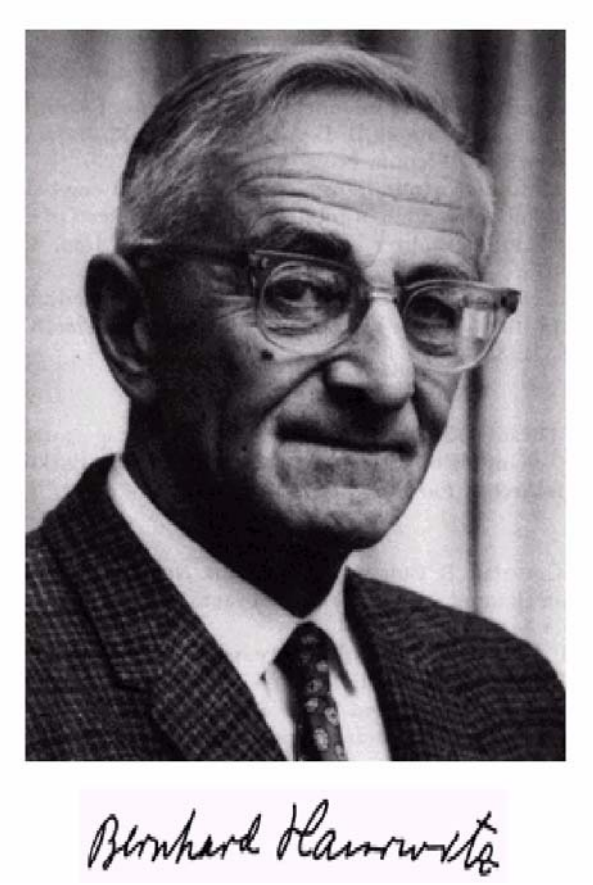

Figure 14.26 Bernard Haurwitz, one of the pioneers of Rossby wave theory.

weather forecasting. Carl-Gustav Rossby (fig. 14.27) developed an elegant approximation known as the β-plane, with which the derivation of the waves is greatly simplified. As so often happens in science, the full force of the earlier theory did not become apparent until long after its discovery. Rossby's influential first paper on the

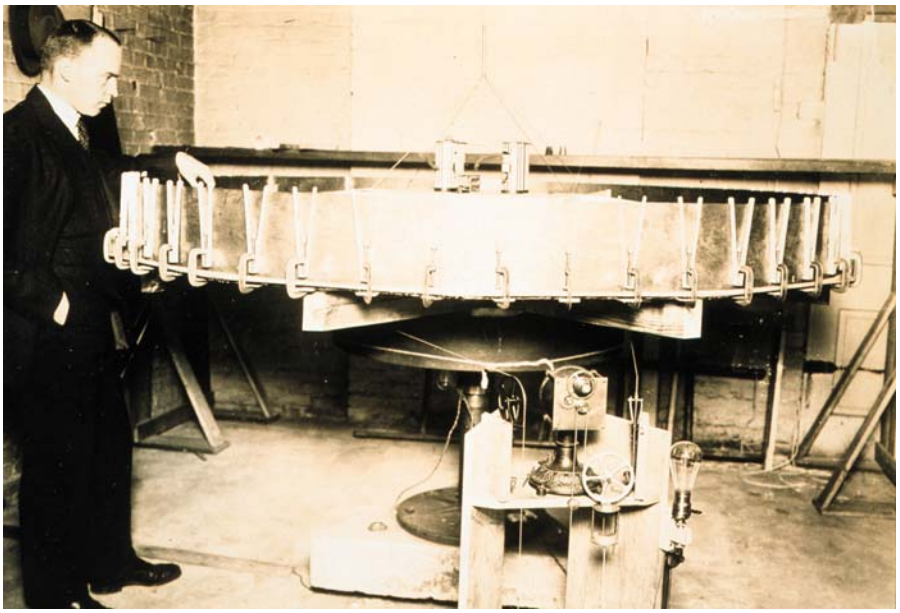

Figure 14.27. Carl-Gustav Rossby in 1926 or 1927, with a rotating platform designed to simulate the Earth's rotation and produce waves and 'weather' (NOAA historic photo archive, http://www.photolib.noaa.gov/historic)

subject appeared in the Journal of Marine Research in 1939 (reminding us that these waves do exist in both ocean and atmosphere). By emphasizing the simple propagation formula Rossby successfully brought the ideas to bear on observations of the circulation. Before the era of computer simulation of the atmosphere, Rossby waves provided a foothold of dynamical theory in aid of weather forecasting. Much later, in the last quarter of the 20th Century, Rossby wave dynamics has filled out, like a powerful flood-light, our understanding of the dark corners of atmospheric dynamics.